P-05-196

Forsmark site investigation

Borehole KFM06A: Characterisation of pore water

Part I: Diffusion experiments

H N Waber
Rock Water Interaction
University of Bern, Switzerland

J A T Smellie, Conterra AB

November 2005

SKB

Forsmark site investigation

Borehole KFM06A:
Characterisation of pore water

Part I: Diffusion experiments

H N Waber
Rock Water Interaction
University of Bern, Switzerland

J A T Smellie, Conterra AB

November 2005

This report concerns a study which was conducted for SKB. The conclusions and viewpoints presented in the report are those of the authors and do not necessarily coincide with those of the client.

A pdf version of this document can be downloaded from www.skb.se

Abstract

Accessible, interconnected pore water has been extracted successfully by laboratory out-diffusion methods from crystalline rocks using some 20 drillcore samples from borehole KFM06A as part of the Forsmark hydrogeochemical site investigation programme. With depth these pore waters generally reflect hydrochemical trends already noted in adjacent formation groundwaters. Insight into the palaeoevolution of the site has been obtained and there is the possibility to use the extraction method to derive rock matrix diffusion coefficients.

Summary

Pore water that resides in the pore space between minerals and along grain boundaries in crystalline rocks of low permeability cannot be sampled by conventional groundwater sampling techniques and therefore has to be characterised by applying indirect methods based on drillcore material. Accessible, interconnected pore water has been extracted sucessfully by laboratory out-diffusion methods using some 20 drillcore samples from borehole KFM06A as part of the Forsmark hydrogeochemical site investigation programme. The objective was to characterise these waters chemically and isotopically and relate these data to the present and past groundwater evolution of the site. In addition, the method of extraction, together with interfaced measurements of interconnected porosity, provides the opportunity to derive diffusion coefficient values of potential use in predicting future rates of solute transport. Because of the very small volumes of pore water extracted, and the possibility of rock stress release occurring during drilling which might lead to contamination by drilling fluid and also affect the derivation of rock porosity values, great care was taken to avoid such problems or, at least further understand the repercussions. Calculations based on hypothetical changes in water content show that a change of 50% caused by stress release would essentially increase the pore water chloride by a factor of 2.

The results show that pore waters were successfully extracted and that the degree of contamination, which is impossible to quantify since the original composition of the pore fluid is unknown, is at a very low level if present at all. The water content porosity, after an initial decrease for the first 200–300 m (~ 0.6 to 0.4 vol %), stabilises at around 450 m and continues uniformly (~ 0.2 to 0.4 vol %) to 1,000 m. Over this distance the pore water appears to change from a shallow, dynamic system Na-Ca-HCO$_3$-Cl type (< 260 m) to a deeper, more stagnant system Ca-Na-Cl type (> 700 m), with an intermediate composition characterised by higher concentrations of Ca, Na, and Cl from 260–700 m depth. These trends generally reflect the major changes in formation groundwater chemistry from adjacent water-conducting fractures and fracture zones. In addition, different species appear to be in steady state with groundwater at different depth intervals (e.g. δ^{18}O in intermediate pore waters and Cl, δ^{37}Cl and Sr-isotopes in deep pore waters). The deeper pore waters also show some affinity with the deep brines of the Canadian basement, for example an increase in chloride accompanied by an increase in δ^{18}O values suggesting prolonged water rock interaction.

At the most shallow depths (100–150 m) the pore water appears to be more saline than the fracture-derived formation groundwaters sampled from the same depth. This trend is reversed down to 600–700 m where the pore water is consistently more dilute than the surrounding formation groundwaters. The greatest disparity occurs to approx 450 m depth where the bedrock is characterised by a high frequency of fractures linked to high transmissivity values. Here the range of pore water δ^{18}O values (–11 to –9.5‰ SMOW) is generally similar to those of the adjacent formation groundwaters considered to be mainly meteoric in origin. Exceptions do occur, for example a pore water at 168.47 m shows δ^{18}O = –15‰ SMOW which suggests a significant cold climate (e.g. glacial melt water) component of unknown age. At depths from approx 400–600 m, where the bedrock is hydraulically tight and the discrepancy in dilution between pore waters and formation groundwaters decreases markedly, δ^{18}O values are generally greater than in the adjacent formation groundwaters although there is some affinity with the brackish, Littorina-type formation groundwaters. At still greater depths (700–900 m), or if the sample has come from a particularly isolated and fracture-free rock matrix horizon at shallower depths, the pore water δ^{18}O values become even heavier (–7 to –5‰ SMOW), representing a

long residence time, brine-type Ca-Na-Cl groundwater environment. At these depths there is a suggestion that the pore water may be becoming more saline than the formation groundwaters; unfortunately there is inadequate formation groundwater data at depth to be more specific.

The $\delta^{37}Cl$ values of the pore water are different (more positive) than those of formation groundwaters from corresponding depths in the upper part of the profile, an observation also noted for the total chloride concentration. Below about 700 m depth the pore water chloride isotope composition is similar to those of the few formation groundwaters sampled. This is further support to suggest a greater active groundwater circulation in the more shallow environments and a situation close to steady state at great depth.

A surprisingly good agreement between calculated pore water and formation ground-water concentrations is observed for strontium. This contrasts with the $^{87}Sr/^{86}Sr$ ratio of the extracted experiment solutions which decreases with depth down to about 700 m as observed for the formation groundwaters, although they are significantly higher than those of the groundwaters. At greater depth a different trend is observed in the $^{87}Sr/^{86}Sr$ ratio of the experiment solutions with some of the values close to those of the formation groundwaters. However, in the absence of rock strontium isotopic data from the Forsmark site these results are difficult to explain. It could be argued that the higher $^{87}Sr/^{86}Sr$ ratios in the experiment solution compared to those of the formation groundwaters are due to more intense water rock interactions during the experiments, although this seems to disagree with the total strontium concentrations. More probably the groundwaters get most of their strontium and $^{87}Sr/^{86}Sr$ ratio from a different source such as the Quaternary sediments overlying the crystalline rocks, while those of the experiment solutions approach the $^{87}Sr/^{86}Sr$ ratio of the rock.

Diffusion has been identified as the dominant process occurring between the water-conducting fractures and the interconnected rock pore system and *vice versa*. In a preliminary exercise the chloride breakthrough curve, monitored during the out-diffusion experiment, has been used to calculate the diffusion coefficient of the rock matrix. The best fit of the measured data is obtained for a pore diffusion coefficient for chloride of about 4.4×10^{-12} m^2/s at a water-content porosity of 0.295%, which agrees with present-day knowledge from the Forsmark site.

Sammanfattning

Det porvatten som existerar i porvolymer mellan mineraler och längs korngränser i kristallint berg av låg permeabilitet kan inte provtas med konventionell provtagningsteknik för grundvatten utan måste karakteriseras genom indirekta metoder baserat på prov från borrkärna. Inom det hydrogeokemiska platsundersökningsprogrammet i Forsmark har tillgängligt porvatten i sammanbundna porvolymer extraherats med hjälp av utdiffusionsmetoder. Omkring 20 borrkärneprov från borrhål KFM06A användes för studien. Syftet var att karakterisera dessa vatten kemiskt samt med avseende på isotopsammansättning och relatera erhållna data till grundvattnets utveckling på platsen i nutid och bakåt i tiden (tillbaka till senaste istid). Dessutom ger extraktionsmetoden, med tillhörande mätningar av den tillgängliga porvolymen möjlighet att erhålla värden på diffusionskoefficienter som kan användas för att förutsäga framtida transporthastigheter i berget. Eftersom de extraherade porvattenvolymerna är mycket små, finns risk att tryckavlastning på borrkärnematerialet under/efter själva borrningen kan förorsaka spolvattenkontaminering från det vatten som finns runt borrkärnan vid borrningen. Eventuell expansion i samband med tryckavlastning kan även påverka härledningen av kärnans porositetsvärden. Därför vidtogs alla åtgärder för att om möjligt undvika sådana problem eller för att i varje fall förstå deras återverkningar. Beräkningar baserade på hypotetiska förändringar i vatteninnehåll visar att en förändring på 50 % orsakad av tryckavlastning skulle öka kloridhalten i porvattnet med en faktor två.

Resultaten visar på lyckade extraktioner av porvatten med liten eller ingen kontaminering, även om kontamineringsgraden är svår att kvantifiera eftersom den ursprungliga sammansättningen på porvattnet är okänd. Efter en initial minskning under de första 200–300 m (~ 0,6 to 0,4 vol %) stabiliserar sig den sammanbundna (vattenfyllda) porositeten vid 450 m borrhålslängd och fortsätter därefter oförändrat (~ 0,2 to 0,4 vol %) ner till 1 000 m borrhålslängd. Över denna distans verkar porvattnet förändras från ett ytnära dynamiskt system av Na-Ca-HCO$_3$-Cl typ (< 260 m) till ett djupare och mer stagnant system av Ca-Na-Cl typ (> 700 m), med en mellanliggande sammansättning som karakteriseras av förhöjda koncentrationer av Ca, Na och Cl i intervallet 260–700 m borrhålslängd. I stort sett reflekterar dessa trender de huvudsakliga förändringarna av grundvattenkemin hos formationsvattnet i näraliggande vattenförande sprickor och sprickzoner. Dessutom verkar olika specier befinna sig i *steady state* med grundvatten vid motsvarande längdintervall (exempel ∂^{18}O i mellanintervallet och Cl, ∂^{37}Cl och Sr-isotoper i djupa porvatten). De djupare porvattnen visar också viss släktskap/samhörighet med de djupa salta vattnen (brine) i den Kanadensiska sköldplattan, tillexempel tyder en ökning i kloridhalt åtföljd av en ökning i ∂^{18}O värden på långvarig växelverkan mellan vatten och berg.

Närmare ytan (100–150 m vertikaldjup) verkar porvattnet ha högre salinitet än formationsgrundvatten härstammande från sprickor provtagna vid samma djup. Sedan är trenden omvänd ner till 600–700 m. Här är porvattnet genomgående mer utspätt än omgivande formationsgrundvatten. Den största skillnaden uppstår vid ca 450 m djup där berggrunden karakteriseras av en hög sprickfrekvens tillsammans med höga transmissivitetsvärden. De ∂^{18}O värden som erhållits vid detta djup (–11 to –9,5 ‰ SMOW) liknar, generellt sett, dem i omgivande formationsgrundvatten som anses vara av meteoriskt ursprung. Undantag finns dock, tillexempel visar ett porvatten vid 168,47 m, ∂^{18}O = –15 ‰ SMOW vilket tyder på ett signifikant bidrag av en "kallt klimat" komponent (glacialt smältvatten) av okänd ålder. Vid djup från ca 400–600 m, där berggrunden är hydrauliskt tät och skillnaden i utspädning mellan porvatten och formationsgrundvatten minskar markant, är ∂^{18}O värdena generellt högre än i omgivande formationsgrundvatten även om det finns viss likhet med bräckt

formationsgrundvatten av Littorina-typ. Vid ytterligare större djup (700–900 m), eller om provet har tagits från ett särskilt isolerat och sprickfritt avsnitt av bergmatrisen på mindre djup, blir $\partial^{18}O$ värdena ännu tyngre (–7 to –5 ‰ SMOW) och representerar ett grundvatten av Ca-Na-Cl brinetyp med lång uppehållstid. Vid dessa djup finns tecken på att porvattnet blir mer salt än formationsgrundvattnet. Olyckligtvis finns inte tillräckligt mycket grundvattendata från dessa djup för att det ska gå att vara mer specifik.

Värdena på $\partial^{37}Cl$ för porvattnen är olik (mer positiva) motsvarande värden för formations-grundvattnen på motsvarande djup i den övre delen av profilen. En observation som också gäller för den totala kloridkoncentrationen. Under ca 700 m djup liknar klorisotopsamman-sättningen den hos proven på formationsgrundvattnet. Detta ger ytterligare stöd för antagan-det om en mer aktiv grundvattencirkulation i den ytnära omgivningen och en situation nära *steady state* vid stort djup.

En förvånansvärt bra överensstämmelse mellan beräknade koncentrationer i porvatten och koncentrationer i formationsgrundvattnen kan iakttas för strontium. Kvoten $^{87}Sr/^{86}Sr$ hos de extraherade experimentlösningarna däremot, minskar med djupet ner till ca 700 m på samma sätt som observerats hos formationsgrundvattnen men de är signifikant högre än grundvattenkvoterna. Vid större djup observeras en avvikande trend i $^{87}Sr/^{86}Sr$ kvoterna för experimentlösningarna där några kvoter ligger nära motsvarande grundvattenkvoter. I avsaknad av isotopdata från bergmaterialet i Forsmark är emellertid dessa resultat svåra att förklara. Det kan göras gällande att de högre $^{87}Sr/^{86}Sr$ kvoterna i experimentlösningarna jämfört med dem i formationsgrundvattnen beror på mer uttalad växelverkan mellan vatten och berg under experimentets gång men detta motsägs av de totala strontiumkoncentra-tionerna. Det är dock mer troligt att grundvattnen får det mesta av sitt strontium och därmed också sina $^{87}Sr/^{86}Sr$ kvoter från en annan källa som exempelvis de kvartära sediment som täcker det kristallina berget, medan kvoterna i experimentlösningarna närmar sig $^{87}Sr/^{86}Sr$ kvoten hos berget i fråga.

Diffusion har identifierats som den dominerande processen mellan vattenförande sprickor och det sammanbundna porsystemet i berget och *vice versa*. I en preliminär övning har genombrottskurvan för klorid under utdiffusionsexperimentet använts för att beräkna diffusionskoefficienten hos bergmatrisen. Bästa anpassningen till uppmätta data erhölls med en pordiffusionskoefficient för klorid på ca $4,4 \times 10^{-12}$ m^2/s vid en sammanbunden (vattenfylld) porositet på 0,295 %, vilket överensstämmer med nuvarande kunskap från platsundersökningarna i Forsmark.

Contents

1 Introduction

This document reports performance and results of the activity *characterisation of pore water* in drillcore samples within the site investigation programme at Forsmark /SKB 2001/. The drillcore samples originated from the drilling of the telescopic borehole KFM06A /Claesson and Nilsson 2005/. The controlling document for the activity is given in Table 1-1.

Crystalline rocks are characterised in general by two hydraulic regimes. The first regime includes the water-conducting zones related to regional or local fracture networks. The second regime includes the bedrock mass of low permeability between the water-conducting zones. Depending on the residence time of formation groundwater in the water-conducting zones, interaction with water present in the pore space of the low permeable bedrock might become significant. In addition, since repository construction will be restricted largely to bedrock of low permeability, this pore water over time will interact with the repository barrier materials (e.g. bentonite; canister) potentially leading to a deterioration in their physical properties. For safety assessment considerations it is therefore important to know the composition of such pore water and its evolution over recent geological time, certainly during the last thousands to hundreds of thousands of years in accordance with the expected lifespan of a repository. Pore water compositions can be assessed by combining the information gained from pore water profiles over bedrock of low permeability with the chemical and isotopic data of formation groundwaters circulating in the adjacent fracture zones.

Pore water that resides in the pore space between minerals and along grain boundaries in crystalline rocks of low permeability cannot be sampled by conventional groundwater sampling techniques and therefore has to be characterised by applying indirect methods based on drillcore material. Such techniques have been tested during the Matrix Fluid Chemistry Experiment in the Äspö HRL /Smellie et al. 2003/ and borehole KSH02 from the Oskarshamn site investigation /Waber and Smellie 2004/. One of these techniques, the laboratory out-diffusion method, has been applied to borehole KFM06A at Forsmark in an attempt to trace the pore water chemistry in low permeable bedrock to depths of around 1,000 m. To achieve this, a total of 20 drillcore samples have been selected at approximately 50 m intervals in fracture free crystalline rock.

Table 1-1. Controlling documents for performance of the activity.

Activity plan	Number	Version
Pore space groundwaters in low permeable crystalline rock	AP PF 400-04-070	1.0

2 Materials and methods

From borehole KFM06A 23 drillcore sections were received between June 22nd and September 22nd 2004 for pore water characterisation. The sections of about 20–50 cm in length were taken at regular depth intervals of approximately 50 m (for details see AP PF 400-05-070). This protocol required the samples to be taken from homogeneous, non-fractured bedrock volumes at least 5 m away from any water-conducting fractures or fracture zones. To safeguard against the selection of unsuitable samples, which might not be obvious at the time, extra core lengths were taken along the borehole length when good rock properties occurred.

An important requirement for pore water characterisation using rock samples is the preservation of the fully water-saturated state of the rock material immediately following drilling and sampling and during transportation from the site to the laboratory. This precaution is to inhibit possible water-rock interactions induced by exposure of the rock sample to air. To minimise these potential perturbing effects the samples were immediately wiped clean with a dry towel following drilling and selection, wrapped into a heavy-duty PVC bag which was repeatedly flushed with nitrogen, evacuated and heat sealed. This procedure was repeated with a second PVC bag and finally sealed in a plastic coated Al-foil. The samples were then air freighted to the laboratory at the University of Bern, Switzerland, where they were immediately stored at 4°C in a cooling room and prepared for the various measurements and experiments within about 20 hours after arrival.

Once exposed to the air and/or stored over too long a time period, the drillcore samples lose their value for pore water characterisation. Therefore, all samples received had to be rapidly conditioned so that the different laboratory experimental procedures could be initiated. For the out-diffusion experiments this involved all the drillcore samples collected (some 23).

In December 2004 a final decision was made as to: a) which three rock samples representing the main rock units in the Forsmark area would be selected for the full analytical programme, i.e. pore water determination plus full mineralogical, geochemical and fluid inclusion characterisation, and b) which samples involved in the on-going out-diffusion experiments were considered unsuitable (e.g. areas of high fracture frequency) or at least potentially problematic for future interpretation. This selection initially was based on a personal on-site drillcore inspection, use of available drillcore mapping information, BIPS logs and also hydraulic data from downhole differential flow measurements. Guidance of the field personnel was invaluable. In January 2005, the three representative samples for a complete mineralogical and geochemical characterisation including fluid inclusion studies were finally agreed upon by the team.

2.1 Samples and sample preparation

For legibility reasons the sample labelling adopted in this report is a subsequent numbering of the samples with depth using the borehole name as prefix; similar labelling was used for the laboratory studies. The conversion of this sample description to the SKB sample number and the depth along borehole is given in Table 2-1. The analytical programme performed on the rock samples and experiment solutions is given in Table 2-2.

Following arrival at the laboratory the core sections were cut by dry sawing into full-diameter samples of about 19 cm length to be used specifically for the out-diffusion experiments. The remaining material from the top and bottom of the core section was used for the isotope diffusive-exchange method and the determination of the water content. For these methods the outer rim of the core (~ 0.5 cm) was first removed by chisel and hammer to minimise any small-scale sample effects resulting from de-saturation during initial perturbations by drilling activities and subsequent sample preparation. The wet weight of such material was determined immediately after preparation. The remaining rim material was further prepared for mineralogical and geochemical investigations.

Table 2-1. KFM06A borehole: list of samples used for pore water studies.

LAB Sample No	SKB Sample No	Depth interval along borehole (m)	Average depth along borehole (m)	Average vertical depth (m)	Date sampled
KFM06A-1	SKB 008550	145.90–146.25	146.07	126.50	21.06.04
KFM06A-2	SKB 008551	194.53–194.85	194.70	168.62	22.06.04
KFM06A-3	SKB 008552	252.22–252.60	252.41	218.59	23.06.04
KFM06A-4	SKB 008553	281.63–282.01	281.82	244.06	23.06.04
KFM06A-5	SKB 008554	298.33–298.65	298.49	258.50	28.06.04
KFM06A-6	SKB 008555	355.14–355.44	355.29	307.69	29.06.04
KFM06A-7	SKB 008556	395.13–395.57	395.35	342.38	30.06.04
KFM06A-8	SKB 008557	440.80–441.15	440.98	381.90	01.07.04
KFM06A-9	SKB 008558	499.85–500.18	500.02	433.03	17.08.04
KFM06A-10	SKB 008559	563.21–563.55	563.38	487.90	19.08.04
KFM06A-11	SKB 008560	575.77–576.11	575.94	498.78	19.08.04
KFM06A-12	SKB 008561	594.43–594.80	594.62	514.96	23.08.04
KFM06A-13	SKB 008562	633.38–633.73	633.56	548.68	24.08.04
KFM06A-14	SKB 008563	660.69–661.09	660.89	572.35	25.08.04
KFM06A-15	SKB 008564	696.61–697.00	696.81	603.46	27.08.04
KFM06A-16	SKB 008565	763.39–763.79	763.59	661.29	31.08.04
KFM06A-17	SKB 008566	810.68–811.00	810.84	702.21	01.09.04
KFM06A-18	SKB 008567	851.56–851.86	851.71	737.60	07.09.04
KFM06A-19	SKB 008568	900.77–901.16	900.97	780.26	13.09.04
KFM06A-20	SKB 008569	920.50–920.87	920.69	797.34	14.09.04
KFM06A-21	SKB 008570	948.58 –948.96	948.77	821.66	15.09.04
KFM06A-22	SKB 008571	977.19–977.53	977.36	846.42	20.09.04
KFM06A-23	SKB 008572	998.13–998.51	998.32	864.57	21.09.04

2.2 Analytical methods

Bulk density (ρ_{bulk}) was determined on sample cubes of about 1 cm^3 from the core centre by the Hg-displacement method. The sample cubes were then ground to < 60 μm and the grain density (ρ_{grain}) was measured by He-pycnometry.

The water content was determined by the gravimetric determination of the water loss by drying subsamples at 105°C until stable weight conditions (± 0.002 g). If the material received allowed it, then the weight of these samples was chosen to be more than about 200 g to minimise de-saturation effects and to account for variations in the grain size of the rocks.

The water content was also determined on the material used for the isotope diffusive-exchange method using the same technique. These samples remained saturated throughout the experiment because they were placed in a vapour-tight vessel at 100% humidity during the equilibration procedure (see also below). The water-content porosity was calculated from the water loss and the grain density measured by He-pycnometry.

A measure for the bulk density of the rocks investigated was also obtained from the volume and saturated mass of the core samples used for out-diffusion experiments. The volume was calculated from measurements of height and diameter of the core samples using a vernier calliper with an error of ± 0.01 mm. Variations in the core diameter over the lengths of the samples was found to be less than 0.05 mm for most samples and a constant diameter was used in the calculation of the volume. For the so-derived wet bulk density this results in an error of less than 3%.

The stable water isotope composition of the pore water was determined by the isotope diffusive-exchange method as originally described by /Rogge 1997/, /Rübel 2000/ and /Rübel et al. 2002/. In this method the isotope exchange occurs through the gaseous phase without any direct contact between the rock sample and the test water. Rock pieces of about 1 cm in diameter from the centre of the core and a small petri dish filled with a test water are stored together in a vapour-tight glass container. The mass and stable water isotope composition of the test water are known. In the test water about 0.3 mol NaCl are dissolved to lower the water vapour pressure above the test-water surface. This is to avoid loss of test water from the petri dish and condensation on the rock fragments and the glass container walls. The petri dish with the test water and the whole container are weighed before and after the exchange experiment to check that no water is lost from the container and there was no transfer of test water to the sample by possible swelling of the rock material. Equilibrium in the three reservoir system – rock sample, test water, and the air inside the container as a diaphragm – is achieved in about 10 to 20 days at room temperature depending on the size and water content of the rock pieces. After complete equilibration the test water was removed and analysed by ion-ratio mass spectrometry.

The isotope diffusive-exchange method was originally designed for rocks with water contents in the order of several percent. To account for the much lower water content in the crystalline rocks of borehole KFM06A, the method was modified in that an artificial test water was used, which is strongly enriched in ^2H and depleted in ^{18}O ($\delta^{18}O = -109.84‰$ and $\delta^2H = +425.5‰$ V-SMOW). This modification was necessary in order to obtain a modified test water composition after equilibration that is outside the standard analytical error of the mass-spectrometer. Obviously, solutions so much enriched in ^2H are difficult to analyse for δ^2H and certain memory effects cannot be excluded for some of the samples. In contrast, the oxygen isotope data are more reliable.

Out-diffusion experiments were performed on complete core samples of about 190 mm in height by immersion into the same artificial test water as used for the isotope diffusive-exchange method (Figure 2-1). To accelerate the out-diffusion, the vapour-tight PVC containers were placed into a water bath with a constant temperature of 45°C. The weight of the core sample, the experiment container, and the artificial test water used was measured before and after the experiment to ensure that no loss of test water has occurred during the entire experiment. Weighing of the core before and after the experiment in addition gives valuable information about the saturation state of the core at the beginning of the experiment.
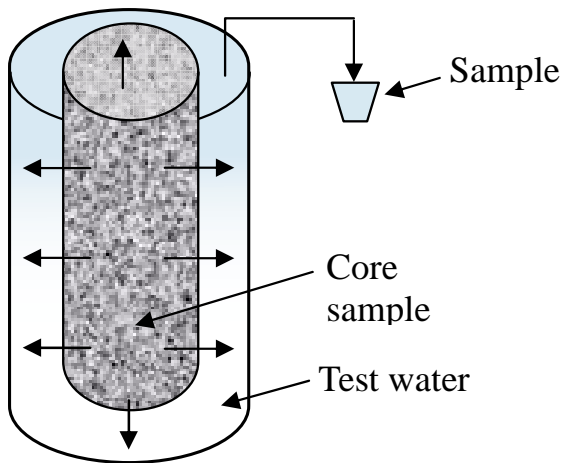
Figure 2-1. *Schematic picture of out-diffusion experiments performed.*

At specific time intervals, initially a few days and later a few weeks, 0.5 mL of solution were sampled for the determination of the chloride concentration as a function of time. The small samples were analysed by ion-chromatography using a 0.2µL injection loop at the University of Bern. The analytical error of these determinations is about 5% based on multiple measurements of the standard solutions.

After steady state with respect to chloride was achieved, the core was removed from the container and the solution was immediately analysed for pH and alkalinity (by titration). The remaining solution was split into different aliquots for chemical and isotopic analyses. Major cation and anion were analysed by ion-chromatography at Hydroisotop GmbH with a relative error of 5%.

The isotopic compositions of oxygen and hydrogen in the various test solutions (diffusive-exchange method, and out-diffusion experiments) were determined by conventional ion-ratio mass spectrometry at Hydroisotop GmbH. The results are reported relative to the V-SMOW standard with a precision of $\pm$ 0.15‰ for $\delta^{18}O$ and $\pm$ 1.5‰ for δ^2H.

The $^{87}Sr/^{86}Sr$ isotope ratio was measured at the University of Bern using a modified VG Sector® thermal ionisation mass spectrometer (TIMS) in simple collector mode, using oxidised Ta filaments. The analytical uncertainty is given with 2σ of multiple measurements of the same sample. Total Sr concentrations are given in ppm.

The $^{37}Cl/^{35}Cl$ isotopic ratio, expressed as $\delta^{37}Cl$ relative to SMOC, was measured at the University of Waterloo Environmental Isotope Lab (EIL) using a VG SIRA 9 Mass Spectrometer. Measurements were made with a precision of $\pm$ 0.15% (1σ) based on repeat analyses of SMOC.

Table 2-2. KFM06A borehole: Experiments and analyses performed on drillcore samples and experiment solutions.

Sample	Isotope diffusive exchange	Out-diffusion experiment	Water-content porosity	Physical porosity	Mineralogy, geochem, fluid Incl. [1]	Aqueous leaching [1]	Chloride time series [1]	pH and alkalinity	Anions and cations	δ18O, δ2H	δ37Cl	87Sr/86Sr
KFM06A-1	X	X	X				X	X	X	X	X	X
KFM06A-2	X	X	X				–	X	X	X	X	X
KFM06A-3	X	X	X				–	X	X	X	X	X
KFM06A-4	X	X	X				X	X	X	X	X	X
KFM06A-5	X	X	X				–	X	X	X	X	X
KFM06A-6	X	X	X				X	X	X	X	X	X
KFM06A-7	X	X	X	X	X	X	–	X	–	X	–	–
KFM06A-8	X	X	X				O	X	X	X	X	X
KFM06A-9	X	X	X				O	X	X	X	X	X
KFM06A-10	X	X	X				O	X	X	X	X	X
KFM06A-11	X	X	X				X	X	X	X	X	X
KFM06A-12	O	O	X	X	X	X	O	X	–	–	–	–
KFM06A-13	X	X	X				O	X	X	X	X	X
KFM06A-14	O	O	X				O	X	–	–	–	–
KFM06A-15	X	X	X	X	X	X	X	X	X	X	X	X
KFM06A-16	X	X	X				O	X	X	X	X	X
KFM06A-17	X	O	X				O	X	–	X	–	–
KFM06A-18	X	X	X				O	X	X	X	X	X
KFM06A-19	X	X	X				O	X	X	X	X	X
KFM06A-20	X	X	X				O	X	X	X	X	X
KFM06A-21	X	X	X				O	X	X	X	X	X
KFM06A-22	X	X	X				O	X	X	X	X	X
KFM06A-23	X	X	X				X	X	X	X	X	X

X = experiment performed; analyses available.
O = experiment performed; analytical data not produced based on final sample selection.
– = not performed.
[1] data will be reported in a different report.

17

2.3   Data handling

Calculations and interpretations are described in connection to the separate issues in Chapters 3, 4 and 5 and in more detail in /Waber and Smellie 2004/. All data from this activity are stored in SKB's database SICADA, where they are traceable by the Activity Plan number.

2.4   Noncomformities

The activity has been performed according to the activity plan without any significant nonconformities.

3   Petrophysical properties of the rock

The characterisation of pore water in rocks of very low permeability and low water content requires knowledge of the water-accessible porosity. This is simply because the pore water in such rocks cannot be sampled directly, but has to be accessed by indirect methods, which all include a dilution of the in situ pore water present. Extensive reviews of this problem and of presently available techniques with their advantages and draw-backs are given in /Pearson 1999/, /Sacchi and Michelot 2000/, /Sacchi et al. 2001/, /Pearson et al. 2003/ and /Smellie et al. 2003/.

Petrophysical measurements conducted on the drillcore samples from borehole KFM06A include the determination of the water loss by drying at 105°C, bulk and grain density by Hg-displacement and He-pycnometry, respectively, and the determination of the wet bulk density from volumetric and mass measurements. From the obtained values the different types of porosity were calculated. The definitions and nomenclature of the different types of porosity follow those given in /Smellie et al. 2003/ in that the *physical porosity* describes the ratio of total void volume to the total volume of rock, the *connected porosity* is described by the water-content porosity obtained from gravimetric water-loss measurements and the *diffusion porosity* is determined by diffusion experiments.

Perturbation of porosity values measured in the laboratory from those present in situ have two major origins besides the analytical uncertainty. These are desaturation of the core sample during sample recovery and handling, and stress release of the sample due to retrieval from great depth. Desaturation was investigated by comparing the mass of the rock samples before and after the out-diffusion experiments. The influence of stress release was investigated by the isotope diffusive-exchange method, which reveals a water-content porosity independent of stress release and, under favourable conditions, a diffusion porosity.

3.1   Bulk density, grain density and physical porosity

The physical porosity, Φ_{Phys}, of a rock can be calculated from measurements of bulk and grain density according to

$$\Phi_{Phys} = [\ 1-(\rho_\beta / \rho_\gamma] \tag{1}$$

where ρ_β is the bulk density and ρ_γ is the grain density.

As shown in Table A1 (see Appendix), bulk and grain densities measured on three dry drillcore samples are almost identical within the analytical error band. Consequently, the physical porosity calculated from these measurements is of low accuracy. In reality the physical porosity should be at least as high as the water-content porosity because it includes also, besides the connected pore space, the isolated pores in the rock matrix and in minerals (i.e. fluid inclusions). While this seems to be the case for samples KFM06A-7 and –12, the calculated physical porosity is lower than the water-content porosity for sample KFM06A-15 (cf Tables A1 and A2). Improvement could be achieved by a higher accuracy of the analytical techniques, larger samples that account for heterogeneities in the rock texture, and measurements of multiple samples for a statistical approach to allow for rock heterogeneity.

For the large-scale samples used for out-diffusion experiments a measure for their (wet) bulk density could be derived from their saturated mass and volume. It varies between 2.59–2.68 g/cm³ with a relative error of ± 3% for the different samples (Table A1). The saturated mass of these samples was about 1,000 g and thus the wet bulk density values account for variations in mineralogical composition. For samples KFM06A-7, -12, and -15 the wet density is consistent with the dry density measured by Hg-displacement (Table A1).

The weight of the large-scale samples used for out-diffusion experiments was measured on two occasions: a) immediately after unpacking the sample, and b) after termination of the experiments. As shown in Figure 3-1, for all samples the two measurements agreed very well indicating that all samples were saturated at the time of their arrival in the laboratory.
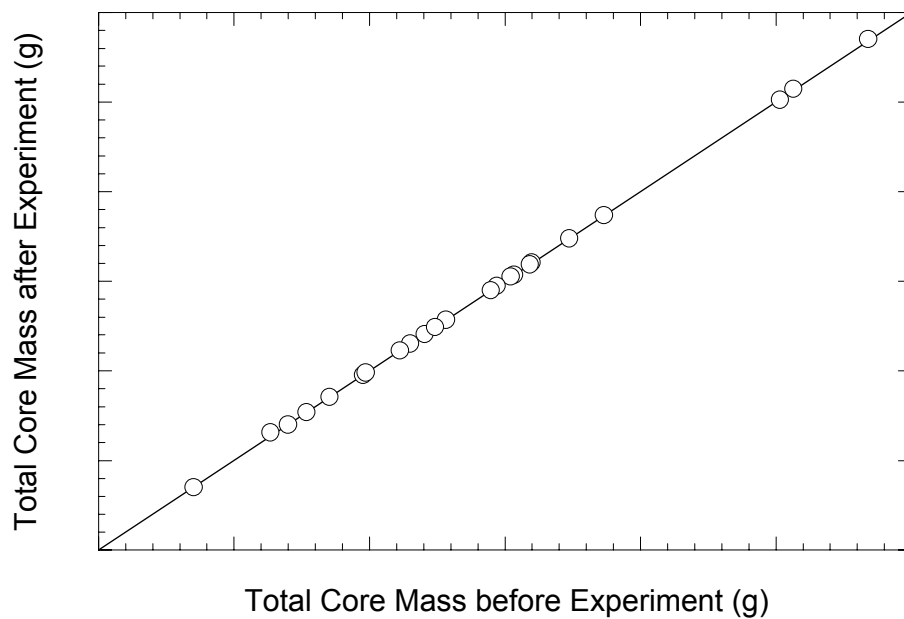
Figure 3-1. *Weight of samples used for out-diffusion experiments before and after the experiment. The identical weights indicate saturation of the sample at the time of arrival in the laboratory (error ± 0.002g).*

3.2 Connected porosity from water-loss measurements

The water content, WC, obtained by gravimetric measurement of the weight loss, WL, by drying the samples at 105°C until stable weight conditions, is given in Table A2, plotted in Figure 3-2 and shown as a function of depth in Figure 3-3. Where possible, the water content was determined for each sample on three subsamples including a large sample specifically assigned to such measurements and the two samples used for the isotope diffusive-exchange method. The mass of the first group of subsamples averaged at 371.25 ± 131.26 g, and that of the second group at 132.23 ± 15.53 g. The standard deviation of the water content is larger for groups of subsamples with lower masses thus reflecting the effect of the textural heterogeneity of the rocks.

Drying time varied between 30 and 105 days depending on the sample size. Figure 3-2 illustrates the decrease in weight during drying for sample KFM06A-21B. The loss of weight with time of this non-fractured sample describes a diffusion-type curve suggesting that the loss of the pore water occurs mainly by diffusion. Unfortunately, the shape of this drillcore sample is not a perfect cylinder in form (i.e. broken ends on both sides) thus hindering a straight forward modelling of the curve obtained.

The water-content porosity or connected porosity, Φ_{WC}, was calculated in two different ways based on the wet weight of the sample. For samples with a known grain density Φ_{WC} is calculated according to:

$$\Phi_{WC} = \frac{WC_{wet} \cdot \rho_{grain}}{WC_{wet} \cdot \rho_{grain} + (1 - WC_{wet}) \cdot \rho_{water}} \tag{2}$$

where WC_{wet} is the water content based on the wet weight, ρ_{grain} is the grain density and ρ_{water} is the density of the pore water (assumed to be 1). Alternatively, for samples with no grain density value available Φ_{WC} is calculated using the wet bulk density, $\rho_{bulk,wet}$, obtained from the samples used for out-diffusion experiments according to:

$$\Phi_{WC} = WC_{wet} \cdot \frac{\rho_{bulk,wet}}{\rho_{water}} \tag{3}$$
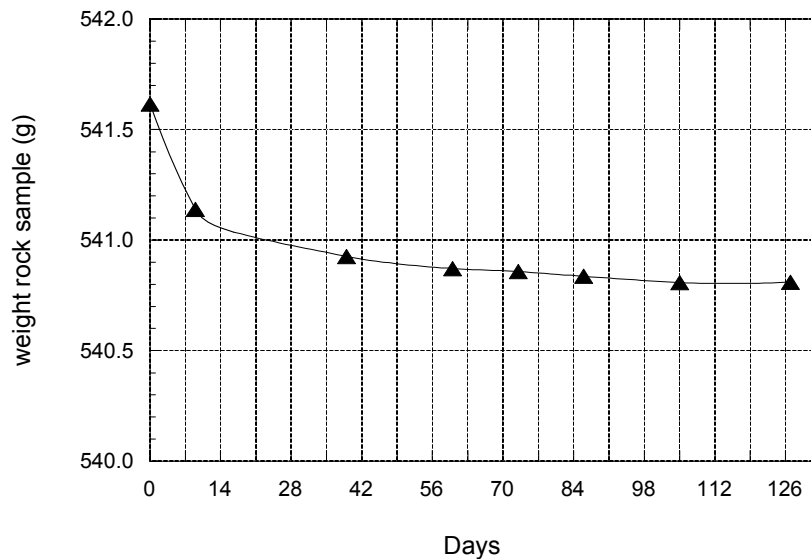
Figure 3-2. *Weight loss of sample KFM06A-21B as a function of time. Initial saturated weight of the sample was 541.616 g; stable weight conditions were achieved after 105 days of drying at 105°C at 540.810 g.*

21

Water content and the connected porosity display a decrease with depth from the surface down to about 450 m of vertical depth whereupon values remain remarkably uniform down to the end of the borehole at around 0.117 ± 0.12 wt.% and 0.306 ± 0.032 Vol %, respectively (Figure 3-3). Samples KFM06A-6 and KFM06A-22 (depths of 307.7 m and 846.4 m, respectively) deviate from this general trend. While this can be explained for sample KFM06S-6 sampled from within a highly tectonised zone with a high fracture intensity, no such explanation applies for sample KFM06A-22, which represents a homogeneous, non-fractured horizon, at least in two dimensions. This overal trend conforms with laboratory measurements of the P-wave velocity, at least to approx 700 m, the maximum depth measured /Chryssanthakis, written comm 2005/.

The measurements of water content and connected porosity of a rock sample can be perturbed by several factors such as non-attainment of stable weight conditions, non-consideration of the rock texture (e.g. too small sample size) or, probably most importantly, stress release of the drillcore sample during drilling or during the experiment. While the first two factors have been considered in the determination of the water content of the present samples, the last deserves more discussion.

Every rock sample recovered from depth is potentially subjected to some stress release. Such release will result in an increase of the void volume of a rock sample and thus perturb bulk density measurements and, if drilled with a drilling fluid, also the water content because some drilling fluid might enter this newly created void volume. It is not well known if stress release in crystalline rocks occurs instantaneously (i.e. during drilling in the borehole) or more slowly over days, weeks, and/or even months. Also, in rocks with such low water content the measurements might simply not be accurate enough to resolve the effects of stress release. While a fully quantitative discussion is difficult with the lack of data at hand, several semi-quantitative arguments can be considered.
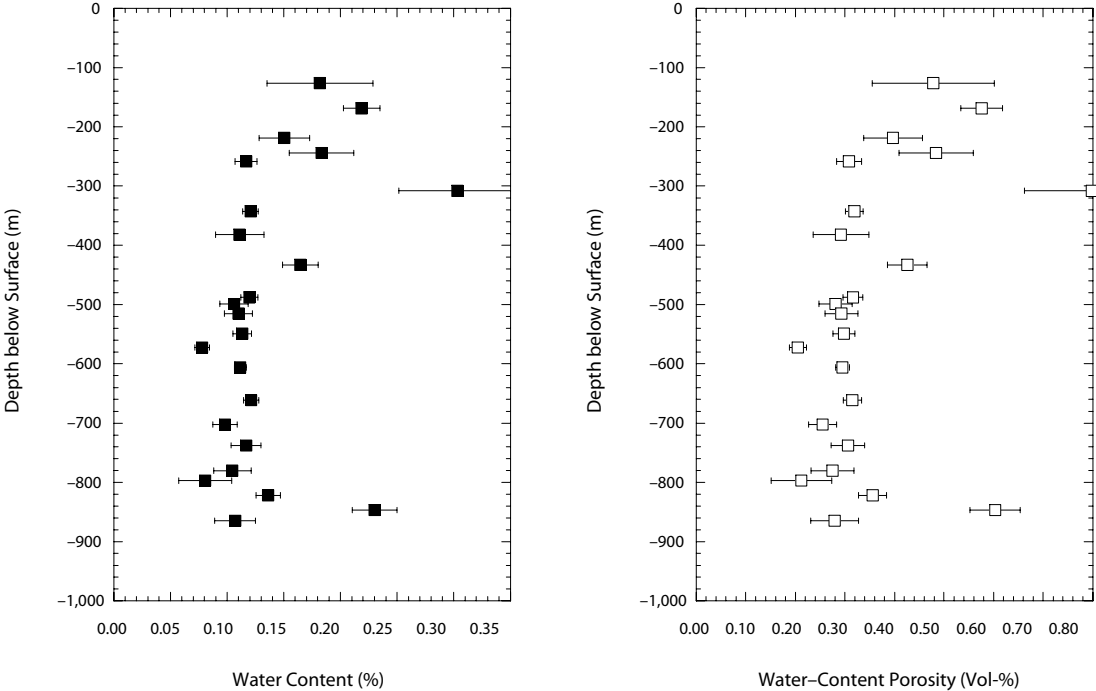
Figure 3-3. *Borehole KFM06A: Water content and water-content porosity of drillcore samples as a function of depth. Note the change in trend at about 450 m depth below surface.*

For borehole KFM06A the highest water contents and connected porosity value are obtained for core samples taken in the first 450 m of depth. This corresponds to the zone with the highest fracture intensity /Mattsson and Keisu 2005/ and the greatest transmissivity /Rouhianinen and Sokolnicki 2005/ (Figure 3-4) which may have undergone already significant stress release due to glacial rebound. The high values obtained are therefore geologically plausible without having to invoke instantaneous stress-release, acompanied by the addition of drilling fluid, during drilling.

In the more deep-seated samples one might expect a greater effect of stress release during drilling (and therefore contamination from drilling fluid) in the core samples because the lithostatic stress increases with depth. However, the cores investigated show remarkably uniform and low values obtained for the water content and connected porosity over a depth interval of more than 500 m (Figure 3-3). If stress release would have affected these samples in a similar way to the shallower samples, then one would expect an increase in the water content with depth. This is not the case; there are no obvious indications from these data that the water content and connected porosity of the studied samples are significantly perturbed by stress release to the extent of introducing significantly high amounts of contaminating drilling fluid.
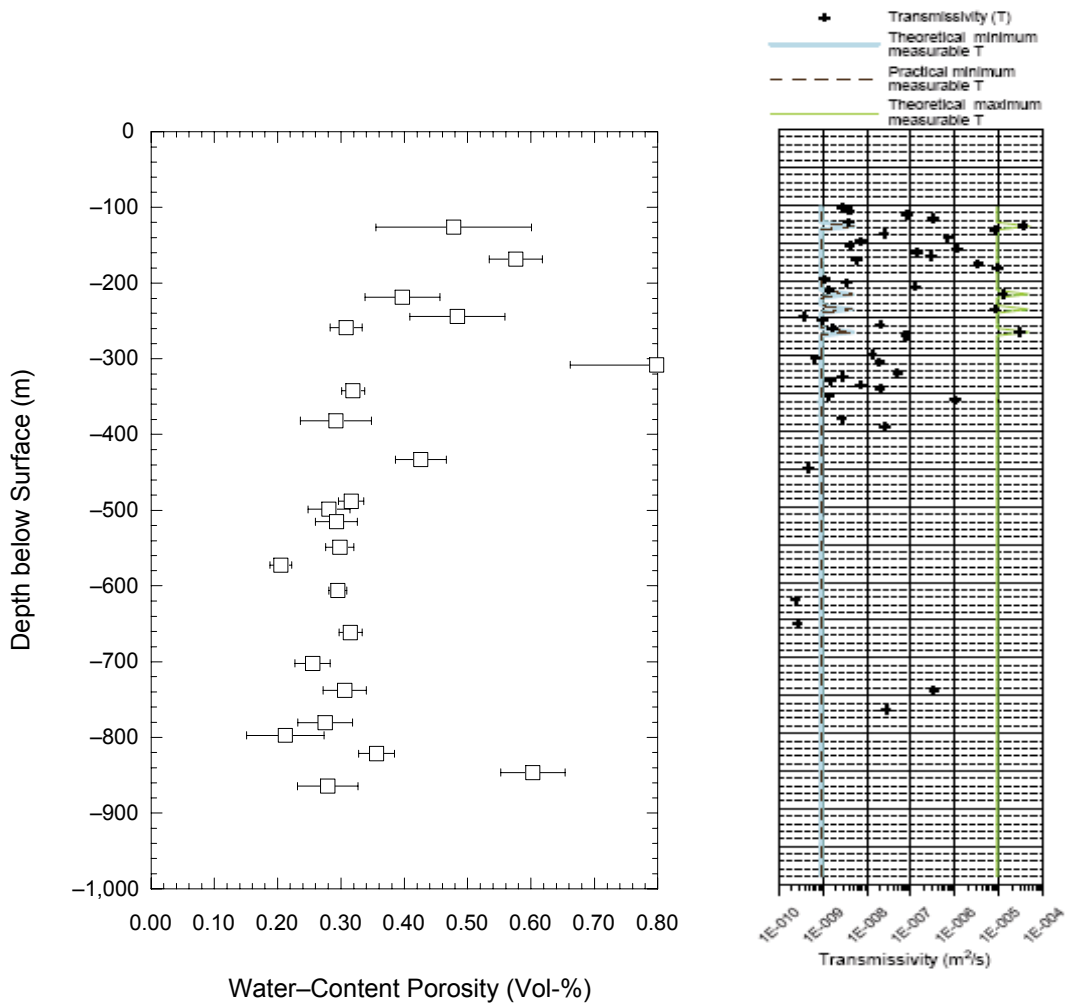
Figure 3-4. Borehole KFM06A: Vertical depth relationship between water-content porosity and transmissivity. (Transmissivity after Rouhianinen and Sokolnicki 2005.)

4 $\delta^{18}O$ and δ^2H of pore water

4.1 Background of the isotope diffusive-exchange method

The diffusive-exchange method for the determination of the stable water isotope composition and the water content of low-permeability rocks was developed by /Rogge 1997/ and /Rübel 2000/. It is based on the concept that the known water isotope composition of a test water will equilibrate with the unknown pore water composition using the gas phase as a diaphragm in a vapour-tight container. The response time τ of the system to completely equilibrate the test water and the pore water is most favourably done from the temporal evolution of either the δ^2H or $\delta^{18}O$ values of the test water by equilibrating several subsamples over different periods of time (time series). Alternatively, the response time τ can be estimated from the relationship:

$$\tau_{total} = \mu/R_{total} \tag{4}$$

where μ is the characteristic mass derived from ratio of mass of test water to mass of pore water and R_{total} denotes the total exchange rate according to:

$$R_{total} = [d^2_{test}/(D_{water} \times m_{tw}) + d^2_{pw}/(D_{water} \times m_{pw}) + 1_{air}/(D_{air} \times \rho_{air} \times A_{air}) \tag{5}$$

where d = distance between the surface of the test water and the surface of the most distant rock piece, D = diffusion coefficient of water, m = mass, r = density, A = cross-section area, tw = test water, and pw = pore water. This latter approach had to be chosen in the present study because the available mass of rock material was limited.

Condensation of the test water on the rock pieces and/or the container walls is minimised by adding NaCl to the test water. As a consequence, one has to consider a difference in the salinity between test water and the (unknown) pore water which results in a slight difference in isotope content of both reservoirs. While there is almost no effect on ^{18}O, the liquid-vapour equilibrium fractionation factor of Deuterium depends on salinity /Horita et al. 1993/. The systematic effect on the result at room temperature is about 2.7‰×ΔM in δ^2H, where ΔM denotes the difference in salinity in mol/kg_{H2O} between solutions. For the KFM06A core samples the difference in salinity is less than about 0.25 mol/kg_{H2O} (see below) and the absolute error from this salinity effect on the δ^2H value is thus lower than 1‰.

The stable isotope composition of the pore water and the water content of the sample is calculated from the mass balance relationship of the experiments according to:

$$m_{pw} \cdot c_{pw}\big|_{t=0} + m_{tw} \cdot c_{tw}\big|_{t=0} = \left(m_{pw} + m_{tw}\right) \cdot c_{tw}\big|_{t=\infty}, \tag{6}$$

where m = mass, c = isotope concentration, pw = pore water, tw = test water and the concentrations on the left side of the equation are prior to equilibration (t = 0), while the concentration on the right side is after equilibration is achieved (t = ∞) in the experiment. Each equilibration experiment reveals two independent equations of the type (6) for $\delta^{18}O$ and δ^2H. To enable the calculation of the three unknowns, i.e. the $\delta^{18}O$ and δ^2H of the pore water and the pore water mass (i.e. the water content), two different exchange experiments have to be performed for each sample to obtain the necessary four equations. It should be noted that at complete equilibration the mass balances remain correct even if a small amount of test water is transferred to the sample during the experiment.

By applying Gauss' law of error propagation, /Rogge 1997/ and /Rübel 2000/ showed that the error of the equilibration experiment for the determination of the isotope composition of the pore water grows with the difference in isotopic composition between test water and pore water. On the other hand, the error of the equilibration experiment for the determination of the water content decreases with the difference in isotopic composition between test water and pore water. Therefore, to minimise the analytical error a test water with $\delta^{18}O$ and δ^2H values close to those expected for the pore water were used for the determination of the isotopic composition and a test water with $\delta^{18}O$ and δ^2H values far from that expected for the pore water was used for the determination of the water content. In the present experiment this was achieved by using laboratory supply water and a synthetic distilled water enriched in ^2H and depleted in ^{18}O. The isotopic composition of the standard solutions are given in Table A3.

4.2. Results

The analytical results of 38 test solutions could be used for further interpretation out of the 42 equilibrated solutions. Two samples must have suffered from evaporation effects as indicated by a consistent enrichment of the heavy isotope according to a Rayleigh distillation process. The experiments are sensitive to an evaporation effect of more than about 3%, which is quite easily achieved at a total test solution volume of 3 mL. Evaporation could have occurred either during the experiment and/or storage of the 3 mL solutions. The δ^2H values of another four solutions were also found to be erroneous. The positive δ^2H values of these are mainly attributed to memory effects during the mass-spectrometric measurement of the test solution initially enriched in ^2H by around 425‰.

Similar effects may also have affected the test solutions of a few other samples to a certain degree. However, there is no obvious analytical and experimental reason to exclude the remaining samples. The water content and pore water $\delta^{18}O$ and δ^2H values calculated from the individual test solutions according to Equation (6) are given in Table A4.

4.2.1 Water content derived by isotope diffusive-exchange

For most samples the water content derived with the isotope diffusive-exchange method, WC_{isoex}, is identical or slightly larger than the gravimetric water content derived by drying, WC_{drying}, (Tables A2 and A4 and Figure 4-1). Only sample KFM06A-2 has a lower WC_{isoex} outside the analytical uncertainty. A higher WC_{isoex} compared to WC_{drying} is explained by the variable electrostatic or steric interactions between the water and mineral surfaces /Horseman et al. 1996, Pearson 1999, Nagra 2002 Chapter 5.4, Pearson et al. 2003. While such interaction is pronounced for clay minerals (up to four layers of water molecules in the diffusive layers) it is less so for carbonates, quartz, and feldspars. Water bound on the mineral surface in the diffusive layers will only be partly released during drying at 105°C. In contrast, this water is believed to undergo isotopic exchange during the isotope diffusive-exchange experiment resulting in the observed difference in water contents. In fact, experiments with claystones revealed that the WC_{isoex} represents the accessible porosity for the diffusion of water which is (significantly) greater than that for dissolved solutes /Nagra, 2002 Chapter 5.4/. The WC_{isoex} derived for the borehole KFM06A samples are therefore geochemically plausible.
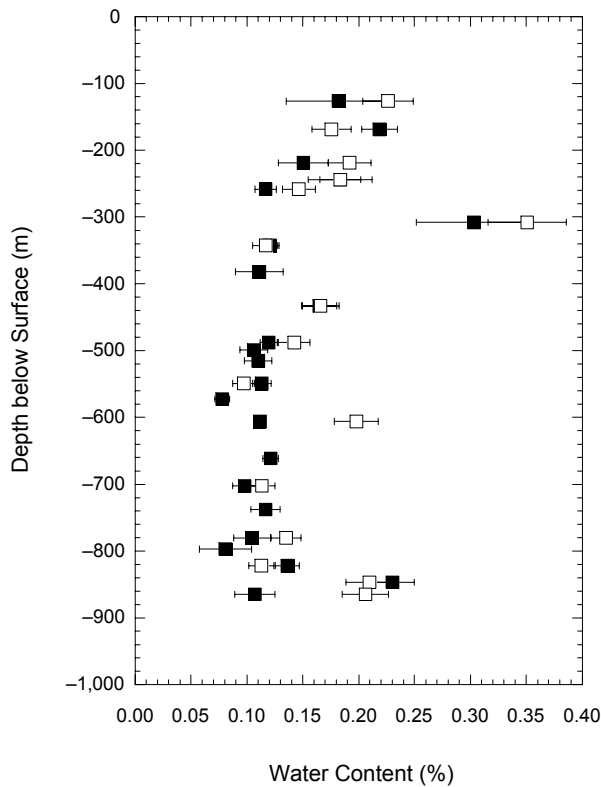
Figure 4-1. *Borehole KFM06A: Vertical depth variation of water content derived by the isotope diffusive-exchange method (open symbols) and by drying (closed symbols). Both methods show essentially the same trends.*

As a function of depth the WC_{isoex}, describes the same general trends as observed from the WC_{drying} (Figure 4-1). Only two samples (KFM06A-15 and KFM06A-23 at depths of 606.1 m and 864.6 m, respectively) have higher WC_{isoex} outside the error band and deviate from this trend. This general agreement is another potential argument against significant stress release affecting these drillcore samples (cf Section 3.2) because the WC_{isoex} represents the porosity accessible for water by diffusion. If significant stress release would have occurred during the drilling process allowing drilling fluid to penetrate into the core samples, this would have to be observed in the water content obtained by the isotope diffusive-exchange method.

4.2.2 Pore water isotopic composition ($\delta^{18}O$ and δ^2H)

The isotopic composition of the pore water is shown in Figure 4-2 and compared with the Global Meteoric Water Line (GMWL) and proposed end-member compositions of various groundwater types /Laaksoharju et al. 1999/. Only the shallow sample KFM06A-2 has a stable water isotope composition with significantly more negative values than present-day precipitation and thus indicating the presence of a cold climate (e.g. glacial melt) compo- nent. Most of the other samples fall to the left of the GMWL with $\delta^{18}O$ values comparable to the reference brine water, but less negative δ^2H values. Such types of isotope composi- tions are known, for example, from crystalline groundwaters in the Canadian Shield /Frape and Fritz, 1987/.
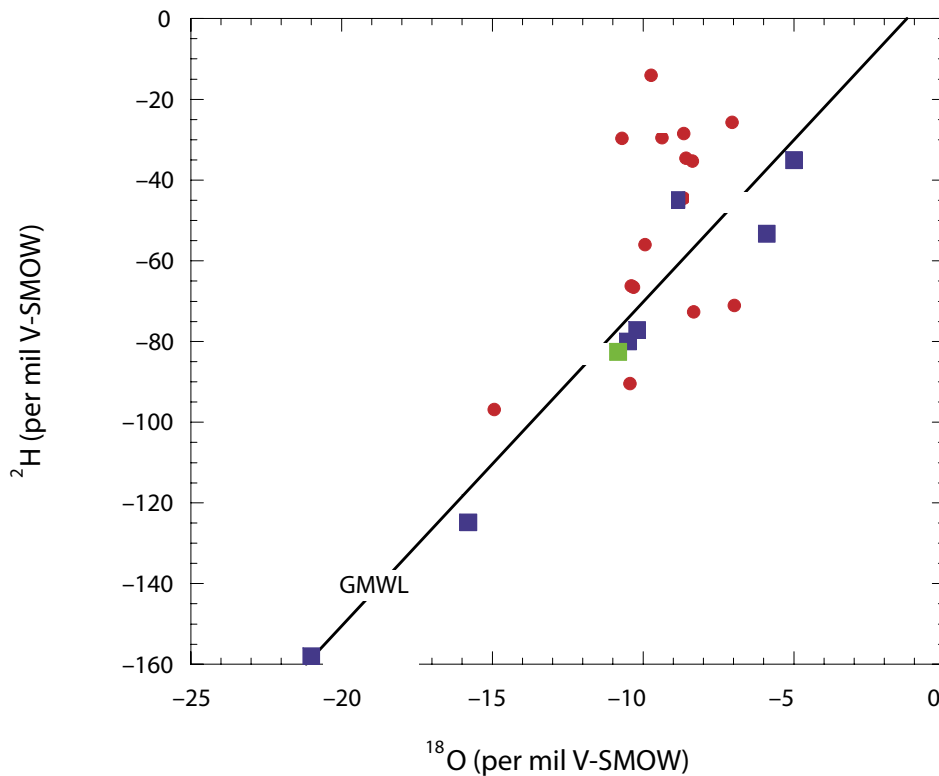
Figure 4-2. *Borehole KFM06A: δ¹⁸O and δ²H values of pore water compared to the GWML and the isotopic compositions of proposed end-member (EM) and reference water (RW) compositions of various Swedish groundwaters /data from Laaksoharju et al. 1999/. The flushing/drilling water (borehole HFM16) is also plotted for reference. Numbers refer to the laboratory samples.*

As mentioned above the calculated δ^2H values are somewhat less reliable than the $\delta^{18}O$ values. Within this context it is interesting to note that the samples with the least negative δ^2H values (KFM06A-6, -15, and -19) show also the greatest differences in the water contents derived by the diffusive-exchange method and by drying (Figure 4-1). This is related to a larger error in the isotope analyses of the traced test water (depleted in ^{18}O and strongly enriched in ^2H; cf Section 2.2) water, which no longer can be resolved.

The three deepest samples have an isotope composition between the brine reference water and present-day meteoric water with two of them (KFM06A-21 and KFM06A-22) plotting on a possible mixing line of brine and glacial water. On the other hand, samples KFM06A-9 and KFM06A-23 suggest more a mixture between some type of marine water and a present-day meteoric and/or glacial water. It is discussed below whether such mixing scenarios based on the isotopic composition are supported by other pore water compounds such as dissolved chloride.

Most of the samples have an oxygen isotope composition of the pore water between –8 to –11‰ relative to V-SMOV and overlap with the isotope composition proposed for the water types A and B (dilute and brackish) as identified and conceptualised from the hydrochemistry of sampled formation groundwater in the area /Laaksoharju (Ed.) 2005/.

Down to about 700 m depth the $\delta^{18}O$ values of the pore water from most rock samples are similar or identical compared to those of sampled formation groundwater (Figure 4-3). Exceptions are a non-fractured interval at about 168 m depth (sample KFM06A-2) and two samples from rather fractured intervals at depths around 499 m and 606 m (samples KFM06A-11 and -15). The shallow sample KFM06A-2 ($\delta^{18}O$ = –14.94‰) was already identified above to have a significant cold climate or glacial component. Samples KFM06A-11 and -15 have $\delta^{18}O$ values greater than –7‰, which compares more to samples below 800 m depth and often typical of the presence of a brine component. From 700–900 m depth most pore water samples have similarly heavy values with again two samples having $\delta^{18}O$ values greater than –7‰ (KFM06A-20 and -23). In contrast to the samples above, however, these samples come from intervals with a higher fracture density. At this depth all samples appear to be significantly more enriched in ^{18}O, albeit compared to the only deep groundwater sample available from the Forsmark site (i.e. from KFM03A).

The pore water $\delta^{2}H$ values do not follow exactly the same pattern as the corresponding $\delta^{18}O$ values (Figure 4-3). While there is general agreement with the groundwater values down to about 200 m and again between 400–500 m, from 200–400 m and below 500 m the pore water $\delta^{2}H$ values are strongly enriched in ^{2}H. The deepest samples show then once again a trend towards more negative $\delta^{2}H$ values. As mentioned above no obvious experimental artefact could be detected that could have altered the $\delta^{2}H$ values in such a (rather accidental) way. On the other hand, however, the obtained data are also difficult to interpret within a general hydrogeological context.
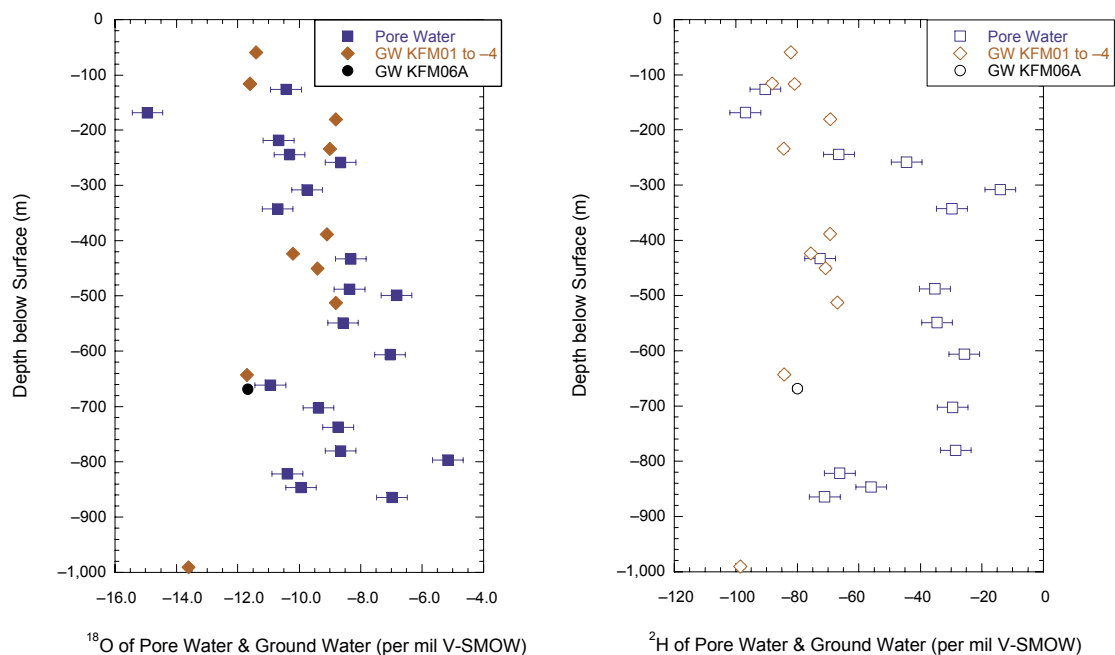
Figure 4-3. *Borehole KFM06A: Vertical depth variation of $\delta^{18}O$ and $\delta^{2}H$ values in pore water compared to groundwater sampled in boreholes KFM01A, KFM02A, KFM03A and KFM04A (data from Table A4 with less reliable values not shown).*

5   Chemical composition of pore water

The chemical composition of the pore water was tackled by applying indirect methods since it cannot be sampled by conventional water sampling techniques. This chapter describes the results of the performed out-diffusion experiments, their implication for the in situ pore water and the derivation of in situ concentrations of chemically conservative compounds.

5.1.   Out-diffusion experiments

Crystalline rocks typically have a low porosity and thus a low pore water content. This requires the use of relatively large rock samples for out-diffusion experiments in order to get: a) a reasonable amount of pore water and thus detectable chemical and isotopic signals, b) an optimised ratio of pore water to experiment solution in order to minimise the analytical uncertainties, and c) to account for the heterogeneity of the rock texture. The second important requirement is the preservation of complete saturation of the rock sample until the start of the experiment. This demands a concerted logistic effort because the drillcore samples have to be packed vapour-tight immediately following recovery, and shipped to the laboratory and processed as quick as possible to minimise possible evaporation and thus loss of pore water and perturbation by chemical reactions.

5.1.1   Experimental set-up

The set-up of the out-diffusion experiments consists of a PE-vessel with a vapour tight cap, which is equipped with two swagelock™ valves and PEEK™ sampling lines. The diameter of the vessel is designed to keep the ratio of experiment solution to rock sample as low as possible, while full immersion of the rock is guaranteed throughout the experiment. Furthermore, the rock sample is placed into the vessel on two small-sized PE-rods to ensure contact with the experiment solution at the lower end of the core. The vessel containing the rock sample and test solution is placed into a water bath and held at a constant temperature of 45°C to accelerate out-diffusion. To avoid chemical stratification of the experiment solution and thus uncontrollable retardation of the diffusion process, the vessels are gently rotated in the water bath throughout the experiment. Three duplicate experiments were run at ambient temperature (20°C) for comparison.

The diameter of the conditioned rock samples varied between 50.1 mm and 50.5 mm with a length of the cylinders between 184.5 mm and 193.5 mm. The corresponding volume varied between 375.424 cm^3 and 392.192 cm^3 with a saturated mass between 987.028 g and 1,036.810 g. The ratio of experiment solution to rock sample was between 0.092 and 0.112.

The experiment solution consisted of distilled water traced with ^{16}O and ^2H and prepared at Hydroisotop GmbH. The chemical composition of the blank solution is given in Table A5 and that of the isotopes in Table A3 (samples STD-TEW 1 to 6).

Steady state conditions of the out-diffusion experiments were controlled by taking small-sized samples (0.5 mL) of the experiment solution at regular intervals (cf Section 5.2). The experiments were terminated and the supernatant solution removed for chemical and isotope analyses when the chloride concentrations had reached a plateau as a function of time, i.e. when steady state conditions were reached. For the experiments run at 45°C this was the case after about 90 days and for those run at 20°C after about 170 days.

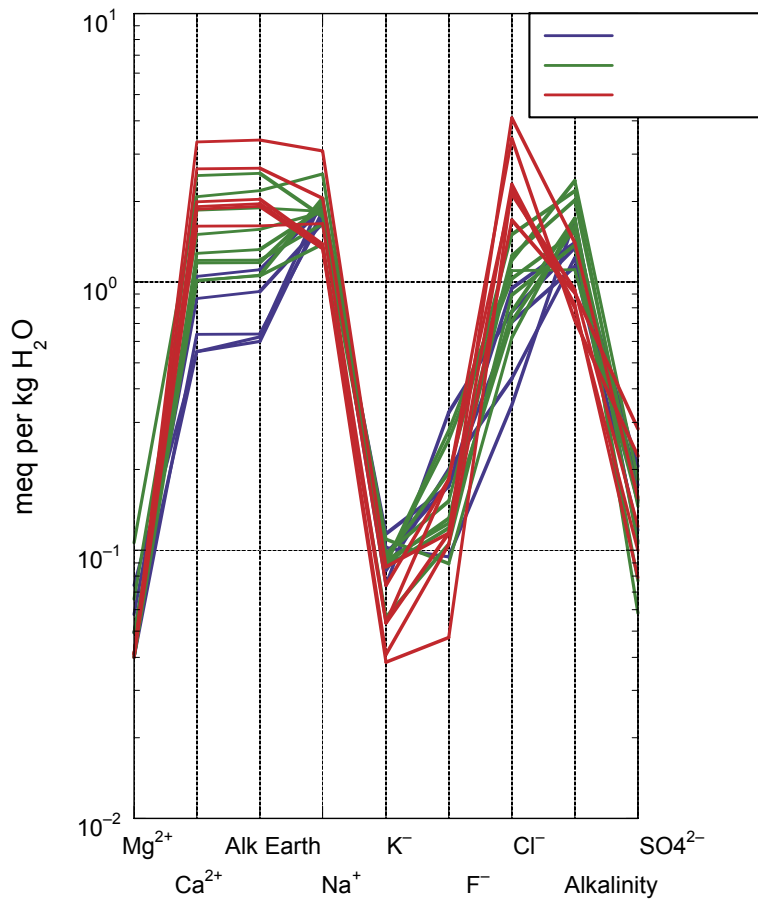### 5.1.2 Composition of experiment solutions

The chemical and isotope compositions of the supernatant solution after termination of the out-diffusion experiments are given in Tables A5 and A6, respectively.

The pH of the experiment solutions varied between 6.10 and 7.74 and the total mineralisation ranged from 158 mg/L to 382 mg/L. The distilled water used as the experiment solution is expected to have acted rather aggressively on the minerals exposed at the drillcore surfaces inducing some mineral dissolution. Mineral dissolution obviously will affect the concentrations of reactive compounds, pH and total mineralisation so that these are not representative for in situ pore water. Major reactions that affect measured elemental concentrations in the experiment solutions involve the dissolution of plagioclase (Ca, Na), K-feldspar (K), biotite (K, Mg), muscovite (K), chlorite (Mg) and possibly fluorite (F), pyrite (SO_4) and calcite (Ca). The high fluoride concentration in some of the solutions suggest that there occurred also some contamination from the polyethylene of the vessels used. Because the general rock mineralogy is rather constant over the entire drillcore, mineral dissolution during the experiments is expected to be similarly uniform. By applying reactive-transport modelling the contribution of mineral dissolution can be quantified; this will be described in a future report when all data become available. Preliminary results of such calculations show that the contribution from mineral dissolution will not significantly alter the general chemical type of the experiment solutions, except for dissolved carbonate. Thus, the chemical type determined on the basis of the experiment solution is qualitatively acceptable as being those of the in situ pore water.

The chemical character of the experiment solutions reveal essentially three groups (Figure 5-1) with the chemical type changing from Na-Ca-HCO₃-Cl to Ca-Na-Cl-HCO₃ at about 700 m vertical depth. Dissolved carbonate in the experiment solution, expressed here as bicarbonate, has occurred to a large degree prior to the experiment since it was in equilibrium with atmospheric pCO₂. While in the first chemical type the dominance of HCO₃ as the major anion is so great that this probably also accounts for the pore water, HCO₃ will disappear as the major anion in the deeper pore waters.

The Na-Ca-HCO₃-Cl-type of experiment solutions can be divided in a group of samples from shallow depth (0 –260 m) with a lower total mineralisation and a group from intermediate depth (260–660 m) with higher concentrations of Ca, Na, and Cl. This could suggest a rather gradual change from the Na-Ca-HCO₃-Cl type to a Ca-Na-Cl-type pore water with increasing depth. However, this preliminary interpretation still has to be confirmed by model calculations.

Chemically conservative elements such as Cl and Br are not affected by mineral dissolution because there are no Cl- and Br-bearing minerals present in the rock. Therefore the concentrations of these compounds can be converted to in situ pore water concentrations using mass balance calculations as is shown below in Section 5.2.

Figure 5-1. *Schoeller diagram of experiment solutions from the drillcore samples showing the change in chemical type and degree of mineralisation as a function of depth. Note that depth is vertical depth below surface.*

5.1.3 Isotope composition of experiment solutions

By using a solution traced in ^{16}O and ^{2}H for the out-diffusion experiments it was initially attempted to obtain information about the water isotope composition of the pore water in an alternative way to the isotope diffusive-exchange method described in Chapter 4. The difference in $\delta^{18}O$ and $\delta^{2}H$ of the experiment solutions before and after out-diffusion of the pore water are well outside the analytical error of the isotope measurements indicating that the traced solution was well designed. However, the calculation of the measured isotope ratios to the in situ pore water ratios requires knowledge of an accurate water content of the rock sample. In addition, the traced experiment solution had initial isotope concentrations that varied greatly from zero. This contrasts with the determination of chloride where the concentration was essentially zero in the initial experiment solution (cf Table A5). Taking these factors together it can be shown that an absolute error in the isotope determination of 1‰, or a relative error in the water content of 1%, results in several tens of per mill difference in the final calculated isotope composition. Therefore, the results given in Table A6 are irrelevant and have been included only for completeness. Such analyses subsequently were abandoned after the first batch of samples were analysed.
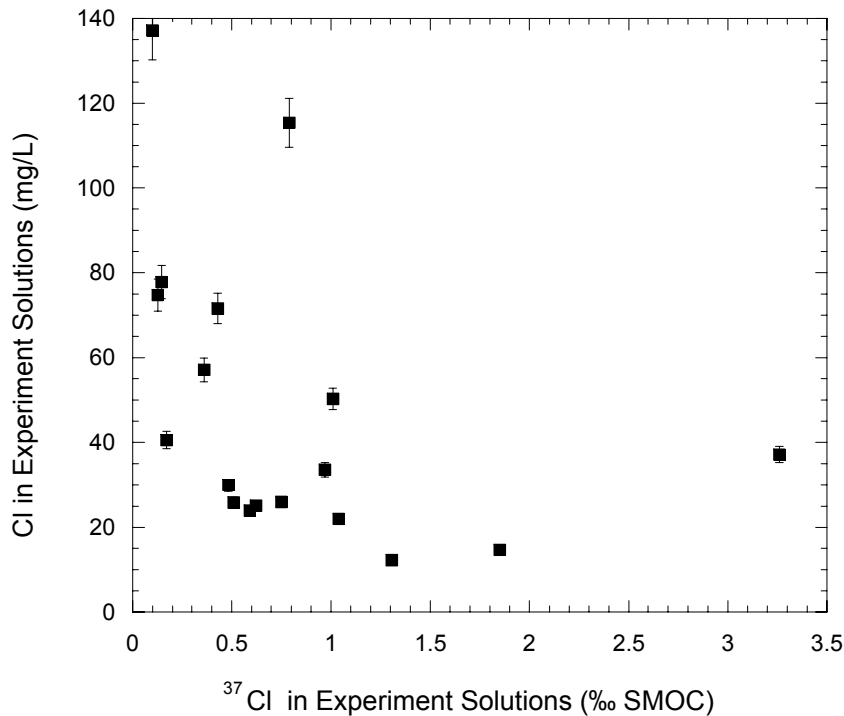
Figure 5-2. *δ³⁷Cl vs. Cl concentration of the out-diffusion experiment solutions of drillcores from borehole KFM06A. A trend towards smaller δ³⁷Cl with higher Cl concentration can be observed (numbers refer to sample numbers).*

The composition of the stable chlorine isotopes, expressed as $\delta^{37}Cl$, has also been determined on the experiment solutions. The $\delta^{37}Cl$ of the experiment solutions fall in the rather narrow range of 0.1–1.5‰ SMOC with only two samples having higher values. There appears to be a trend towards smaller $\delta^{37}Cl$ values with higher Cl concentrations in the experiment solutions (Figure 5-2). The reason for the high $\delta^{37}Cl$ value of sample KFM06A-15 is yet unknown. Such a strong difference from the trends given by all other samples is not observed for any other chemical or isotopic parameter of this sample and there is also no obvious analytical artefact that could be invoked.

It is known that the chlorine isotopes fractionate during the diffusive transport of chloride /Desaulniers et al. 1986, Eggenkamp et al. 1994/. In contrast to other isotope pairs, this fractionation is measurable mainly due to the large difference in the natural abundance of the two isotopes ^{35}Cl and ^{37}Cl. Generic calculations of two-sided diffusion show that the $\delta^{37}Cl$ values in the initial reservoir (in this case the rock pore water) and the bounding reservoir (in this case the experiment solution) will become equal after steady state with total chloride is attained between the two reservoirs /Gimmi and Waber 2003/. The same will account for a radial geometry as in the present experiments. Because steady state was attained for chloride in the experiment solutions (cf Section 5.2), the $\delta^{37}Cl$ values measured in the experiment solutions appear to be representative for the in situ pore water.

In contrast to chloride, strontium is a reactive element and will be involved in mineral dissolution reactions. Depending on the total mineralisation of the in situ pore water the effect of such reactions on the total Sr concentration in the experiment solution will be very small. This is due to the occurrence of Sr as trace element in the minerals and the limited mineral dissolution over the experiment time. In contrast, the effect on the Sr-isotope ratio, $^{87}Sr/^{86}Sr$,

is expected to be much greater. This is because Sr released from the Sr-bearing mineral phases (mainly feldspars) contains most probably much more radiogenic Sr and thus a higher ^{87}Sr/^{86}Sr ratio compared to that of the pore water. The similar petrologic evolution of the rock might suggest that its Sr-isotope composition will range in a rather narrow band. Thus the contribution of Sr with an isotope ratio different from that of the pore water due to mineral dissolution can be expected to be similar for all samples.

Total Sr concentrations, Sr_{tot}, in the experiment solutions are low and vary between 0.068 and 0.597 mg/L (analysed by mass spectrometry). The corresponding ^{87}Sr/^{86}Sr-ratios vary between 0.7153 and 0.7290 (Table A6). The concentrations of Sr_{tot}, of the experiment solutions are positively correlated with those of Cl (Figure 5-3). This supports the above hypothesis in that the concentration of Sr_{tot} in the experiment solution is largely determined by the contribution from the pore water than to that of mineral dissolution. In Figure 5-4 of Sr_{tot} against the ^{87}Sr/^{86}Sr ratio two different trends are established. Samples above about 700 m depth (samples KFM06A-1 to -16) display a negative correlation between Sr_{tot} and ^{87}Sr/^{86}Sr-ratio, while deeper samples below about 700 m (samples KFM06A-18 to -23) display a positive correlation, with sample KFM06A-21 deviating from this trend. Because of the positive correlation between Sr_{tot} and Cl, the same trends are observed between Cl and the ^{87}Sr/^{86}Sr-ratio of the experiment solution with sample KFM06a-21 now conforming better with the general trend (Figure 5-5).

Based on these observations one can conclude that the concentrations of Sr_{tot} in the experiment solution are essentially determined by the pore water, and the ^{87}Sr/^{86}Sr-ratio during the out-diffusion experiment reflects more the pore water than mineral dissolution reactions. Thus, the different trends observed in the ^{87}Sr/^{86}Sr-ratio above and below about 700 m depth indicate differences in the pore water chemistry.
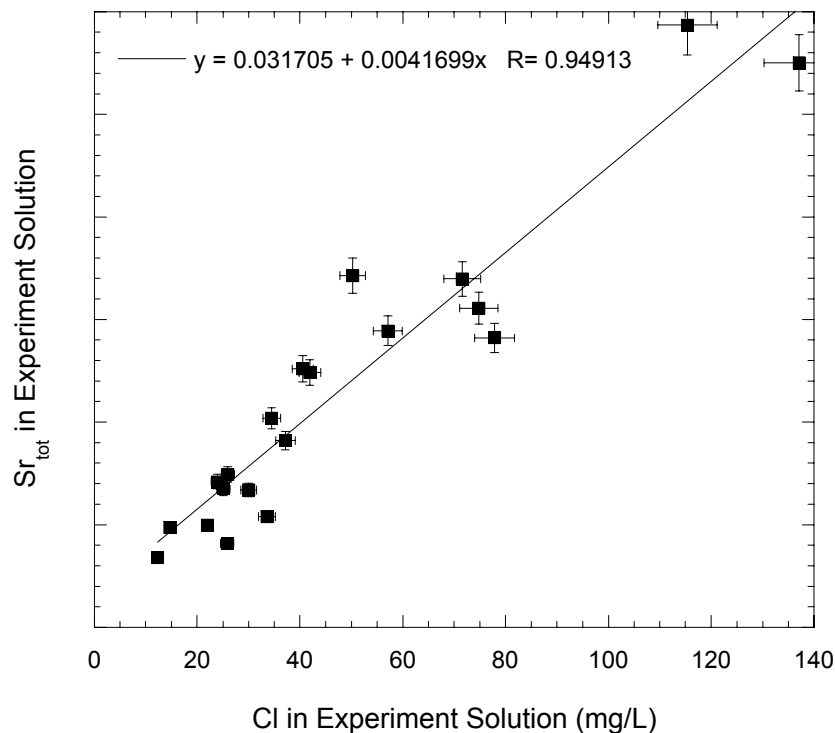
Figure 5-3. Borehole KFM06A: Positive correlation of total strontium concentration, Sr_{tot}, against chloride for the drillcore out-diffusion experiment solutions.
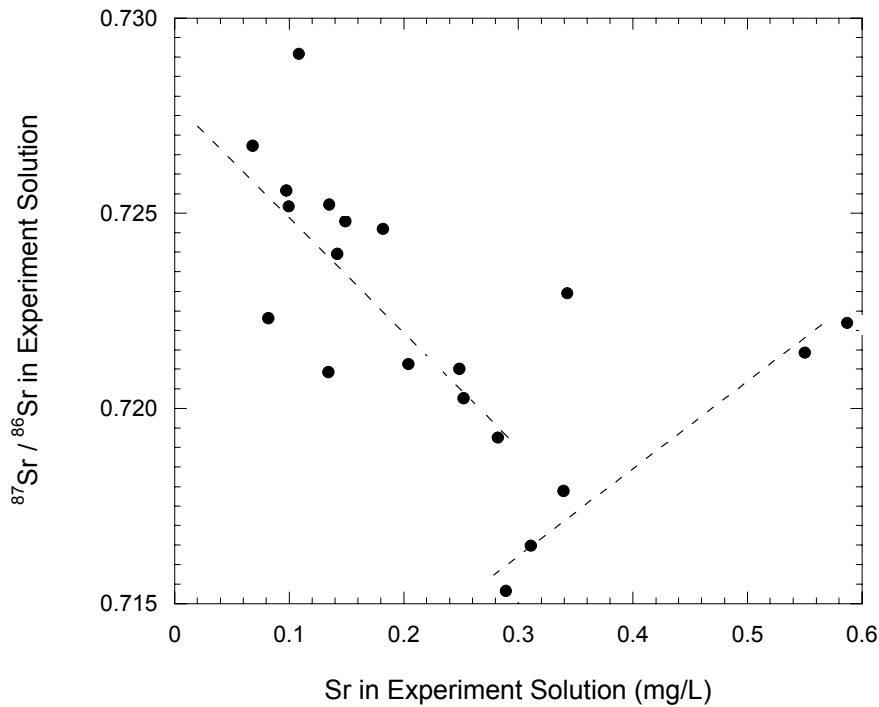
Figure 5-4. *Borehole KFM06A: Strontium isotope ratios ($^{87}Sr/^{86}Sr$) plotted against the strontium concentrations of the drillcore out-diffusion experiment solutions. Two different trends are indicated for samples above (sample numbers 1–16) and below (numbers 18–23) about 700 m depth.*
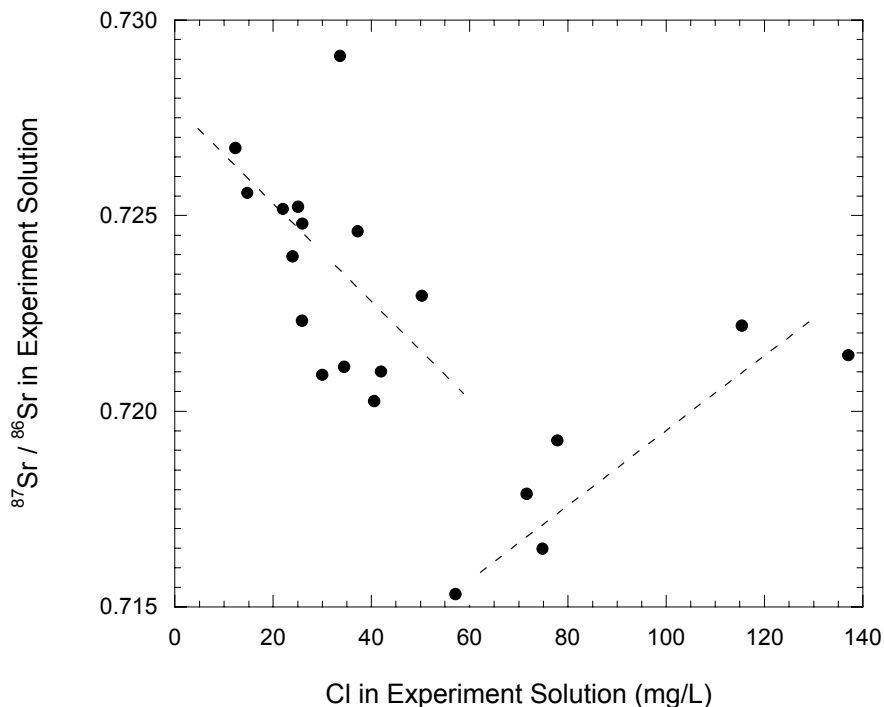
Figure 5-5. *Borehole KFM6A: Strontium isotope ratios ($^{87}Sr/^{86}Sr$) plotted against the chloride concentrations of the drillcore out-diffusion experiment solutions. Two different trends are indicated for samples above (sample numbers 1–16) and below (numbers 18–23) about 700 m of depth.*

5.2 Pore water chloride

The non-reactive behaviour of chloride and the non-destructive nature of the out-diffusion experiments, for example which contrast with crush/leach aqueous extraction techniques, make the pore water the only source for dissolved chloride in the experiment solution. Therefore, the chloride concentration of the experiment solution can be readily calculated to pore water concentrations given that steady state conditions in the out-diffusion experiment are achieved.

5.2.1 Control on steady state: Chloride time series

The monitoring of steady state conditions in the out-diffusion experiments was performed with small-sized samples (0.5 mL) that were taken at regular time intervals and analysed for chloride. Steady state conditions with respect to chloride diffusion is attained when the concentrations reach a plateau, i.e. when they remain constant. Obviously, the analysed Cl concentrations have to be corrected for the volumes of experiment solution that have been systematically removed during the experiment.

The analysis of such small-sized samples is not straight forward. In addition, sample treatment and storage has to be thoughtfully done because the slightest evaporation of the sample will have a strong effect on the attempted final results. Figure 5-6 shows the currently available results of chloride analyses of the 0.5 mL samples taken some 7 days before the termination of the experiment, compared with the larger 40 mL samples taken at the end of the experiment. The analyses were performed in two different laboratories for a quality check. As can be seen from this figure there is excellent agreement between the analyses, which gives great confidence in the chloride time-series measurements.
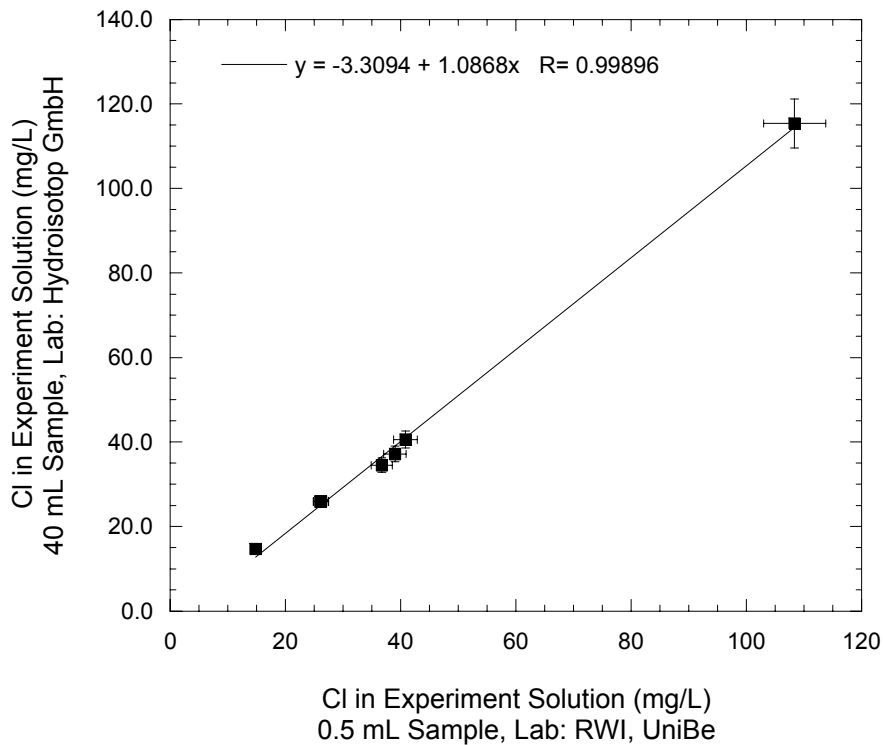
Figure 5-6. *Chloride concentrations of experiment solutions analysed on small-sized 0.5 mL samples and larger 40 mL samples. The analyses performed in two different laboratories show excellent agreement.*

In Figure 5-7 an example of a chloride time series is given to illustrate that steady state conditions with respect to the out-diffusion of chloride were achieved in the experiments. As can be seen from this figure steady state for chloride diffusion in sample KFM06A-15 was already achieved after about 50 days.

5.2.2 Derivation and sensitivity of pore water chloride concentrations

Out-diffusion of the pore water from the drillcore into the surrounding experiment solution has occurred from each surface face of the core as schematically shown in Figure 5-8.

At steady state conditions the chloride concentration in the connected porosity of the rock sample will be equal to that of the experiment solution. With knowledge of the mass of pore water in the rock sample from gravimetric water-content and/or isotope diffusive-exchange experiments (cf Chapter 3), the chloride concentration of the pore water can be calculated according to:

$$C_{PW} = \frac{\left(m_{PW} + m_{TEWi} - \sum_{}^{n} m_S\right) \cdot C_{equil,corrected} - (m_{TEWi} \cdot C_{TEWi}) + \sum_{}^{n} m_S \cdot C_S}{m_{PW}} \qquad (7)$$

with:

$$C_{equil,corrected} = \frac{C_{TEW\infty} \cdot \sum_{}^{n} m_S}{m_{TEWi}} \qquad (8)$$

where C = concentration, m = mass, n = number of samples and the subscripts PW = pore water, TEW = experiment solution, S = small-sized sample taken for chloride time series, i = at beginning of experiment, and ∞ = at end of experiment.
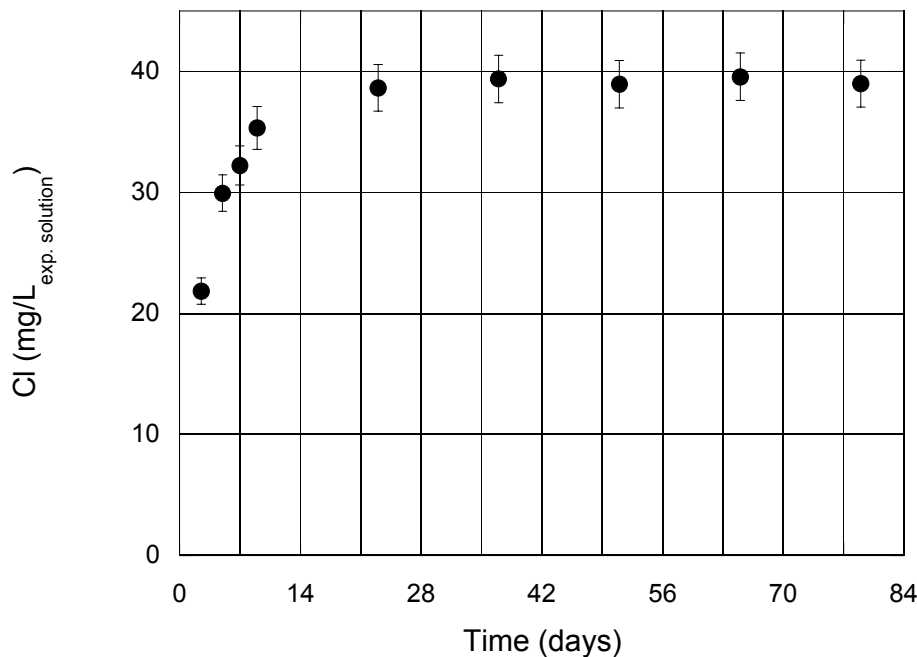
Figure 5-7. *Sample KFM06A-15: Chloride concentrations of the experiment solution as a function of diffusion time (chloride time series). The achieved plateau indicates steady state conditions for chloride diffusion. Chloride concentrations were analysed on small-sized 0.5 mL samples.*

38
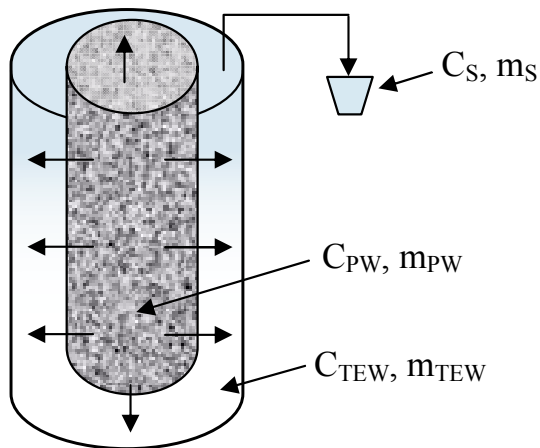
Figure 5-8. *Schematic picture of out-diffusion experiments performed.*

The last term in Equation (7), $\Sigma m_S \times C_S$, describes the amount of chloride removed from the initial experiment solution by the chloride time series samples. The final measured concentration of chloride in the experiment solution, $C_{TEW\infty}$, is corrected for the mass of solution removed by the chloride time series samples from the initial mass of experiment solution, m_{TEWi}, to get the Cl concentration in the experiment solution at steady state, $C_{equil.corrected}$ (Equation 8). The correction for chloride in the initial experiment solution is necessary because this solution was not entirely free of chloride as shown in Table A5. The calculated pore water chloride compositions are given in Table A7.

From Equation (7) it can be seen that the calculated pore water chloride concentration is inversely proportional to the mass of pore water. The mass of pore water is derived from the water content, which can be subjected to various perturbations that can deviate it from in situ conditions. As shown in Chapter 3, different, independent methods applied to determine the water content on samples of different size yield consistent results indicating that significant desaturation of the samples can be excluded as a perturbation. Desaturation would result in a too low water content and consequently in a too high calculated pore water concentration.

Stress release of the rocks is the second possibility to deviate the measured water contents from in situ conditions. Stress could have occurred (or still can occur) continuously and slowly from the time of drillcore recovery to the end of the measurements/experiments in the laboratory and/or it could have occurred instantaneous during drilling in the borehole. In the first case this would result in a desaturation of the rock samples which, as mentioned above, is not observed. In the second case, the newly created pore space would, if connected with the core surface, become filled with the surrounding fluid used for drilling the borehole. Such an effect could not be detected by gravimetric water content measurements. Furthermore, if significant, it should have been detected in the water content determined by the isotope diffusive-exchange method, which seems not to be the case as shown in Chapter 4. Similarly, one would expect to see systematic perturbations in the chemical and isotopic composition of the out-diffusion experiments as a function of their sampling depth. This is because deep seated samples would suffer the strongest stress release and are also in contact with the drilling fluid for the longest duration of time (shallow samples on average 1 hour, deeper samples on average 2 hours). As will be shown below such indications appear to be minimal, if not absent, for the investigated samples.

The behaviour of the samples and experiment solutions during the out-diffusion experiments can also help to argue for or against significant effects induced by stress release. Thus, initial model calculations show that the out-diffusion of chloride from the pore water of the rock into the experiment solution can be described by diffusion as the dominant transport mechanism (see Section 5.2.3). Because the contact time between the drillcore and the drilling fluid was on average in the order of 1–2 hours, this suggests that the effect of possible dilution of the pore water by the less mineralised drilling fluid is very limited and probably outside the resolution of applied methods.

Although it seems that measurable effects of stress release are minimal, the arguments so far are of a qualitative and semi-quantitative character. Therefore the possible effect by potential stress release on the calculated pore water concentration shall be explored further. The effect of possible dilution of the pore water by the less mineralised drilling fluid cannot be explored easily because this depends on the in situ chloride concentration of the pore water, which is unknown. However, a higher pore water chloride concentration would result at steady state conditions in a higher chloride concentration in the experiment solution. As can be seen from Equation (7) this would result in a higher calculated pore water concentration. As mentioned above, the probability of a significant dilution of the in situ pore water seems to be low. In contrast, stress release effects might be masked by the water-content measurements and in reality the in situ water content could be lower than that measured. As a consequence the pore water chloride concentration would be underestimated because of the inverse proportionality of the water content to the pore water chloride concentration (Equation 7). This is shown for two purely hypothetical scenarios in Figure 5-9. There the calculated pore water concentrations are shown for water contents decreased by 30% and 50% to that measured. As can be seen from this figure, the decrease in water content leads to increased pore water chloride concentrations. For a 50% decrease this is an increase by a factor of 2 due to the inverse proportionality of the two parameters.
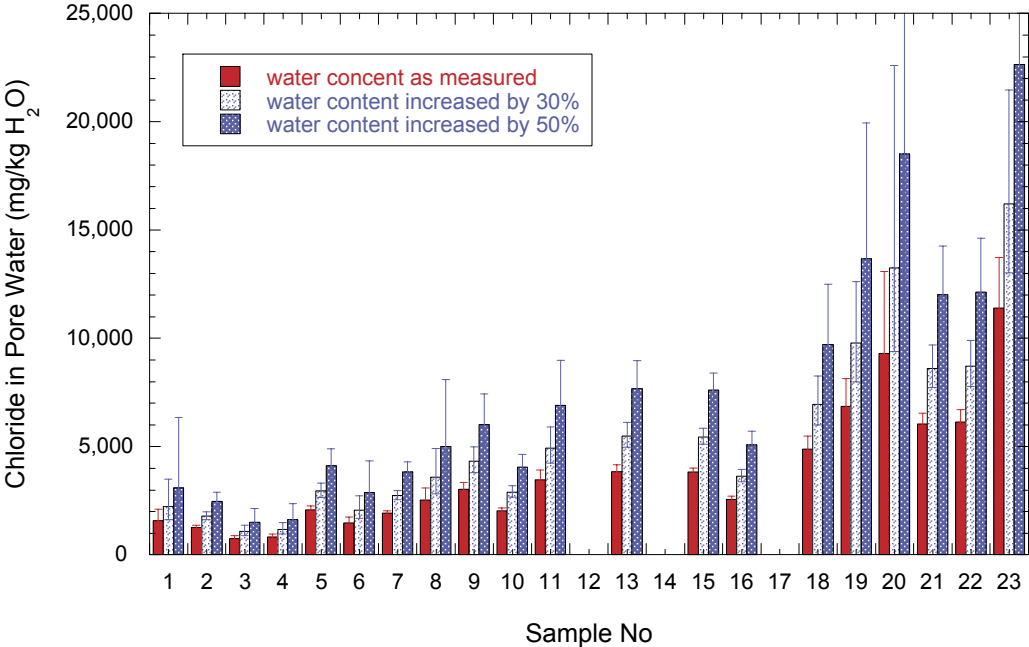

Figure 5-9. *Sensitivity of calculated pore water chloride concentrations with increasing sample number (i.e. depth). Two hypothetical scenarios are shown with water contents decreased by 30% and 50% to that measured due to possible stress release effects. Error bars indicate the cumulated error.*

40

5.2.3 Preliminary modelling of chloride breakthrough

In a preliminary exercise the chloride breakthrough curve of sample KFM06A-15 shown in Figure 5-10 has been modelled using an analytical solution of radial diffusion out of cylinder into a well-mixed solution reservoir /Crank 1975/. In this initial modelling the removal of small-sized samples of experiment solution was neglected in the transient phase, but incorporated in the mass balance for the steady state condition according to Equation (7). In future calculations incorporation of this removal will lead to an improvement of the fit to the measured data.

For sample KFM06A-15 the best fit of the measured data is obtained for a pore diffusion coefficient for chloride of about 4.4×10^{-12} m^2/s at a water-content porosity of 0.295%. This diffusion coefficient is in the same order of magnitude as numerous diffusivity measurements of igneous intrusive rocks. /Löfgren 2004/ obtained effective diffusion coefficients, D_e, for dioritic rocks from the Laxemar area using samples of 15 mm to 50 mm in through-diffusion and through-electromigration experiments. These diffusion coefficients are only lower by a factor of about three compared to that found for the Forsmark granite sample. The same author also shows that the granitic rocks of Forsmark generally have lower formation factors than those of the Laxemar area due to their greater average grain size. Thus, the difference in diffusion coefficients could be accounted for by differences in the formation factor and present results are fully consistent with these previous findings.
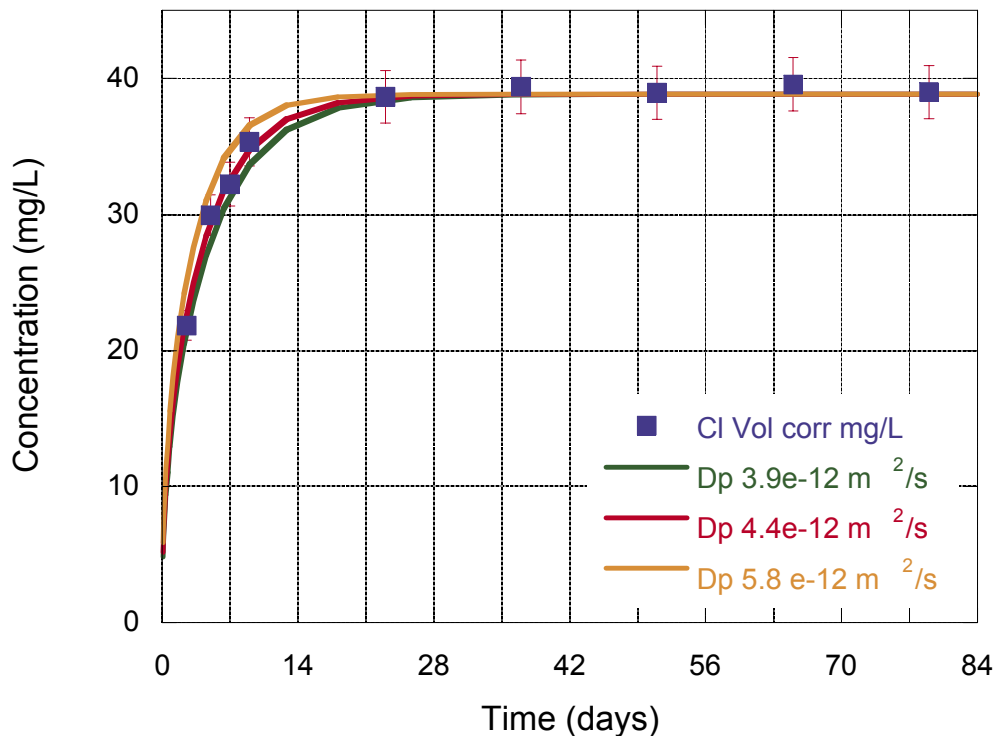

Figure 5-10. *Sample KFM06A-15: Modelling of chloride out-diffusion. The best fit is achieved for a diffusion coefficient D_P of about 4.4×10^{-12} m^2/s.*

5.2.4 Pore water chloride and isotopic compositions

In groundwaters and brines chloride often shows specific relations with certain isotopes which might be indicative for the origin and geochemical evolution of the water. In the current pore waters one might expect similar features because of the possible long residence time of the pore water in the rock. Thus, pore water in low permeability rocks might act as an archive of the palaeohydrological evolution. Yet, it has to be kept in mind that the granitic rocks of the Forsmark area contain an actively circulating groundwater system in their fracture network. The pore water in a non-fractured rock mass will therefore be subjected to interaction with such fracture formation groundwater exactly as observed in the small-scaled out-diffusion experiments. The degree of interaction, and thus the degree of archived palaeohydrological information, depends on the distance between the centre of a low-permeability rock mass to the next fracture(s), the chemical gradient and temperature and pressure. Depending on the duration of the presently active system, signatures of older processes might be completely erased and/or partly imprinted on each other leading to complications in interpreting the observed data.

In crystalline rocks prolonged water rock interaction can lead to a correlated increase in the chloride content and the $\delta^{18}O$ values, such has been documented for highly saline groundwaters and brines in the Canadian Shield /Pearson 1987/. Trends are also observed in the rock pore waters from borehole KFM06A (Figure 5-11). In fact, there appear to be two trends, one for samples down to about 700 m depth and another for samples from greater depths (i.e. samples KFM06A-18 to -23). Only the shallow sample KFM06A-2, with its very negative $\delta^{18}O$ value, appears to be anomalous. The two trends indicated coincide with the change in chemical type from $\underline{Na}$-Ca-$\underline{HCO_3}$-Cl to $\underline{Ca}$-Na-$\underline{Cl}$-HCO$_3$ as observed for the experiment solutions (cf Section 5.1.2). In comparison with the formation groundwater types proposed in the conceptual hydrogeologcial model of the Forsmark area /Laaksoharju 2005/, the shallow $\underline{Na}$-Ca-$\underline{HCO_3}$-Cl pore waters overlap with the dilute, shallow dilute Type
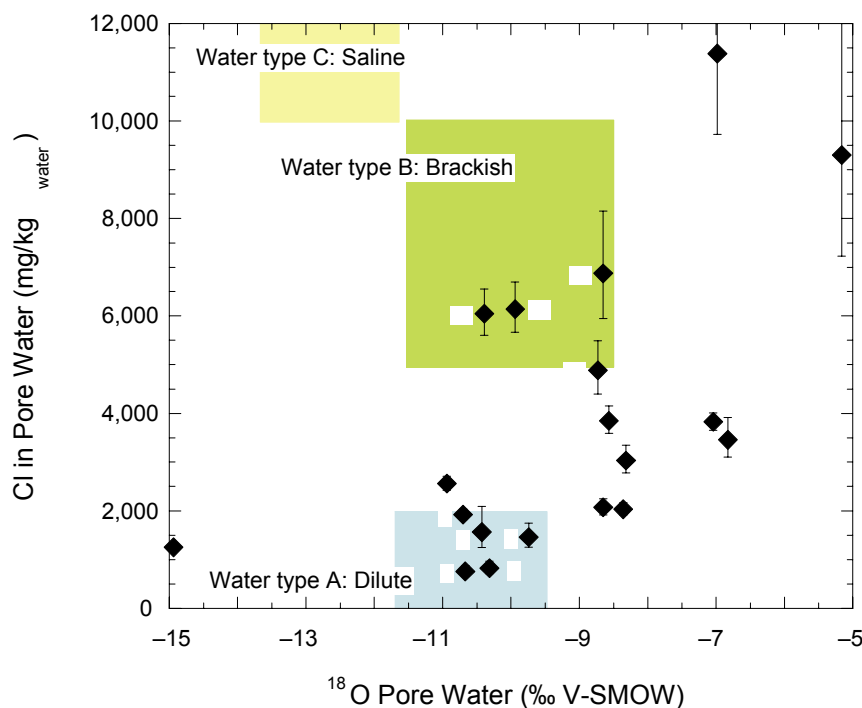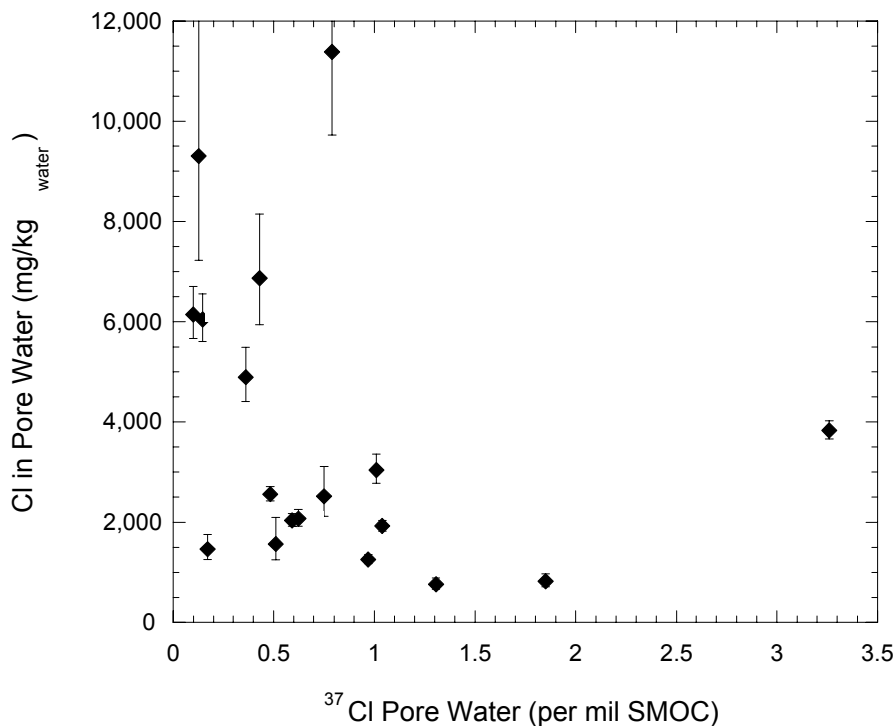

Figure 5-11. *Chloride contents plotted against the $\delta^{18}O$ values of pore water from rocks in borehole KFM06A. The coloured fields demarcate the ranges of different water types given in the conceptual hydrogeological model of the Forsmark area /from Laaksoharju 2005/.*

A groundwaters, while the intermediate pore waters, characterised by higher mineralisation of the experiment solutions, plot between the dilute Type A and the brackish (i.e. Littorina) Type B groundwaters. The deep Ca-Na-Cl type pore waters overlap, in part, with the brackish

Type B groundwaters with the most saline pore water samples having an oxygen isotope composition distinctly more enriched in ^{18}O than the saline Type C groundwaters of the conceptual model. This suggests a significant brine type component in these deep pore waters.

As can be expected from the relation between $\delta^{18}O$ and δ^2H (Figure 4-1) no such trends can be observed between the δ^2H values and Cl concentrations of the pore water. Similarly, no trend is developed for $\delta^{37}Cl$ and Cl in the pore water (Figure 5-12). Although the separation between the Na-Ca-HCO$_3$-Cl and Ca-Na-Cl type pore waters is more pronounced than in the experiment solutions (Figure 5-2) due to the larger separation in Cl concentrations, the $\delta^{37}Cl$ values of the shallower Na-Ca-HCO$_3$-Cl-type cover the whole range of $\delta^{37}Cl$ values. In addition, the hyperbolic relation between Cl and $\delta^{37}Cl$ suggested in Figure 5-11 converts only to a poor linear correlation in a diagram of 1/Cl vs. $\delta^{37}Cl$, which would be indicative for simple mixing of two water types. Therefore, the $\delta^{37}Cl$ values suggest a more complex evolution.

When converted to pore water concentrations, the chloride and the strontium isotope ratios appear to be more linearly related (Figure 5-13) than separating into two groups as was indicated for the experiment solutions (Figure 5-5). Thus, the $^{87}Sr/^{86}Sr$ ratio of the pore water has to be further investigated in combination with the same ratio in the minerals and the minerals dissolving during the out-diffusion experiment. Of special interest would be if the rock strontium isotope signature changes at a depth of about 700 m.

Figure 5-12. Chloride contents plotted against the $\delta^{37}Cl$ values of pore water from rocks in borehole KFM06A (numbers refer to sample numbers).
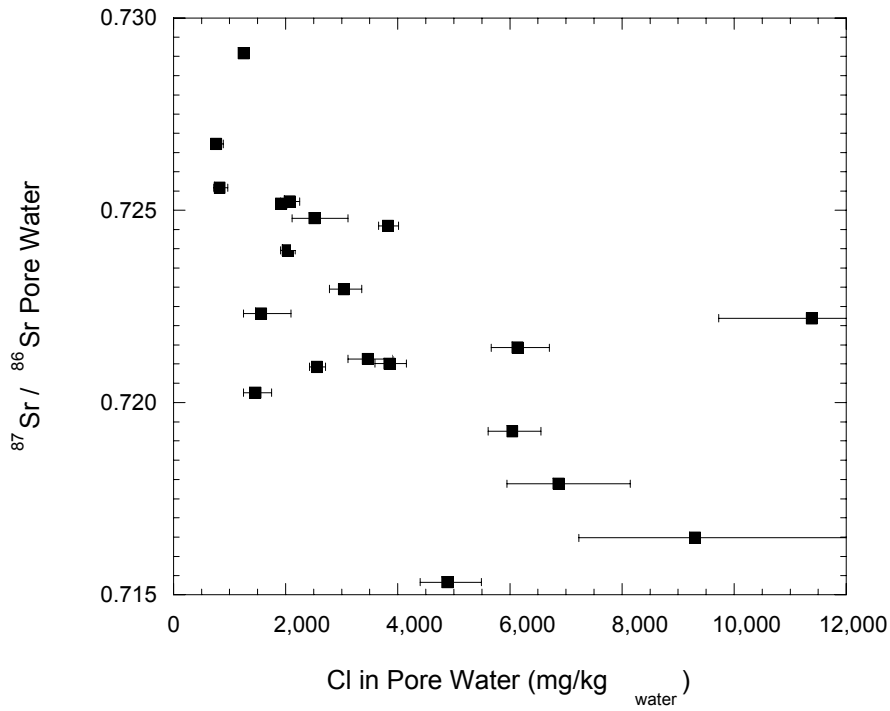
Figure 5-13. *Pore water chloride contents plotted against the [87]Sr/[86]Sr isotope ratio of experiment solutions from out-diffusion experiments of rocks in borehole KFM06A. A more linear trend is observed in contrast to Figure 5-5 (numbers refer to sample numbers).*

6 Comparison of pore-water and groundwater compositions

The unit for the pore water is given as mg/kg H_2O (and not mg/L) because it is derived on a mass basis rather than a volumetric basis. This is because the density of the pore water is not known beforehand. In reality the difference between mg/L and mg/kg H_2O is negligible. Chloride concentrations in the pore water of borehole KFM06A are below about 1,500 mg/kgH_2O down to about 260 m of depth. From there the concentrations increase almost continuously down to a depth of about 700 m. It is below this depth that the change in chemical type also occurs and the chloride concentrations increase to a maximum of almost 12 g/kgH_2O.

The most shallow groundwater samples from fracture zones in boreholes adjacent to borehole KFM06A have lower concentrations than obtained for the pore water (Figure 6-1, left). But already at a depth of 120 m the formation groundwaters, here including also a groundwater of borehole KFM06A /Wacker et al. 2005/, have distinctly higher chloride contents than the pore water. Below about 700 m the pore waters and formation groundwaters have similar chloride concentrations and a situation close to steady state conditions is indicated.

Figure 6-1 (right) also shows the comparison of pore water chloride concentrations calculated with arbitrarily decreased water contents with those of the formation groundwater. As can be seen from this figure, the pore water chloride concentration would remain below those of corresponding formation groundwaters down to a depth of about 350 m. Concentrations in pore water and formation groundwater would be closer between 350 m and about 700 m of depth. Below this depth pore water chloride concentrations would exceed those of the formation groundwaters with the highest contents being about 23 g/kgH_2O. As mentioned in the previous section there are no well-supported arguments for such a large discrepancy between measured and in situ water content at present. Of course, it could be argued that conditions close to steady state in the interval between 350 m and about 700 m would be in agreement with the oxygen isotope composition of pore water and groundwater (cf Figure 4-3). However, this would either neglect the differences in diffusion coefficients for water and chloride or imply a very long time period with the presently prevailing conditions in the groundwater to reach steady state conditions for both these parameters. Such a long time period of constant groundwater conditions at this depth interval seems hardly possible considering the dependence of the groundwater oxygen composition on the climatic conditions during recharge and the fact that groundwaters from this interval still have considerable amounts of atmospheric [14]C.

The $\delta^{37}Cl$ values of the pore water are different (more positive) than those of formation groundwaters from corresponding depths in the upper part of the profile similar as observed for the total chloride concentration (Figure 6-2). Below about 700 m depth the pore water chloride isotope composition is similar to those of the few formation groundwaters sampled. As for chloride this suggests a more active groundwater circulation in the more shallow environments and a situation close to steady state at great depth. This is in agreement with present hydrodynamic modelling results and other hydrogeochemical evidence.
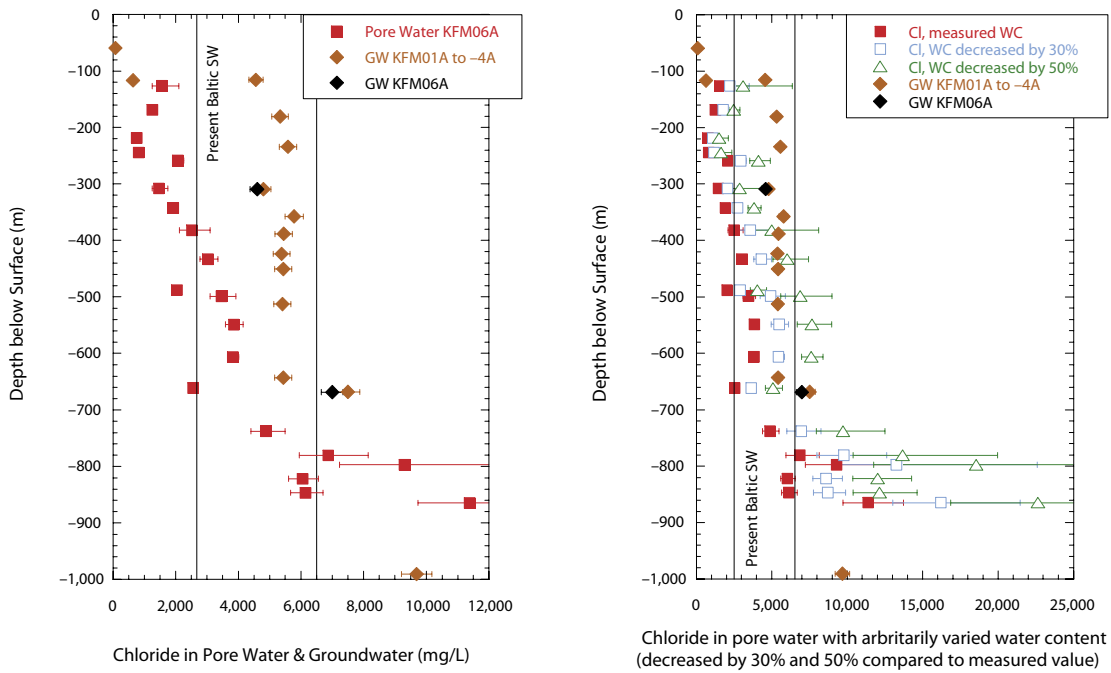
Figure 6-1. *Vertical depth variation of chloride concentrations of rock pore water from borehole KFM06A compared with groundwaters sampled from adjacent fractures (left) and the same comparison with pore water chloride concentration calculated with arbitrarily decreased water contents (right; GW = groundwater, WC = water content).*
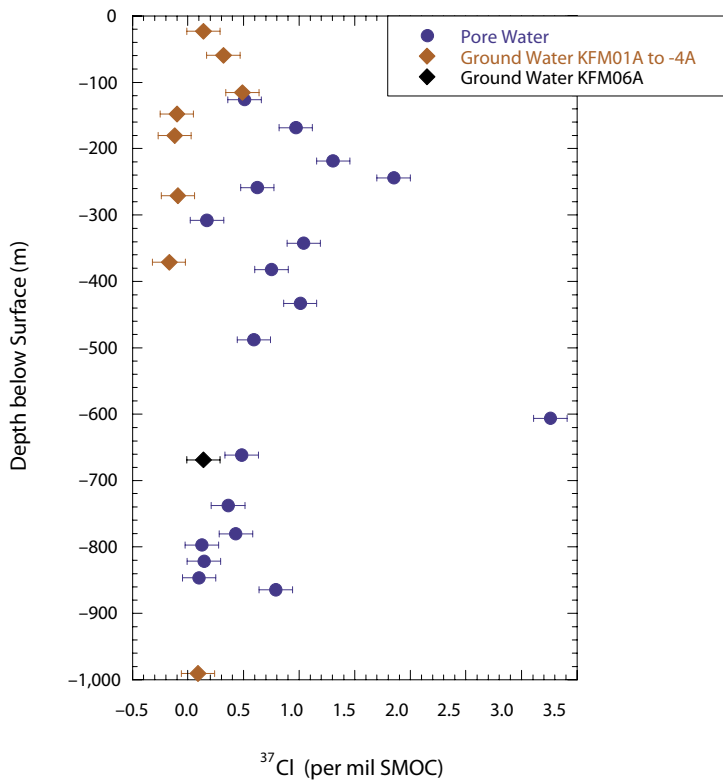
Figure 6-2. *Vertical depth variation of chloride isotope ratios in pore water of rocks from borehole KFM06A compared with those of groundwater sampled from fractures.*

46

A surprisingly good agreement between pore water and formation groundwater concentrations is observed for strontium (Figure 6-3, left). This seems to support the hypothesis made in Chapter 5 that most of the strontium analysed in the experiment solutions is derived from the pore water. As in the groundwater the strontium concentrations increase almost uniformly in the pore water with depth down to about 700 m from where on the increase seems to be greater.

In contrast the $^{87}Sr/^{86}Sr$ ratio of the experiment solutions decreases with depth down to about 700 m in a similar way as observed for the formation groundwaters (Figure 6-3, right). Down to this depth the $^{87}Sr/^{86}Sr$ ratios of the experiment solutions are in general significantly higher than those of the groundwaters. At greater depth a different trend is observed in the $^{87}Sr/^{86}Sr$ ratio of the experiment solutions with some of the values close to those of the groundwaters.

Without having strontium isotope data of the rocks at hand this behaviour is difficult to explain. It could be argued that the higher $^{87}Sr/^{86}Sr$ ratios in the experiment solution compared to those of the groundwaters are due to more intense water rock interactions during the experiments. However, this seems to disagree with the total strontium concentrations. More probably the formation groundwaters get most of their strontium and $^{87}Sr/^{86}Sr$ ratio from a different source such as the Quaternary sediments overlying the crystalline rocks, while those of the experiment solutions approach the $^{87}Sr/^{86}Sr$ ratio of the rock.
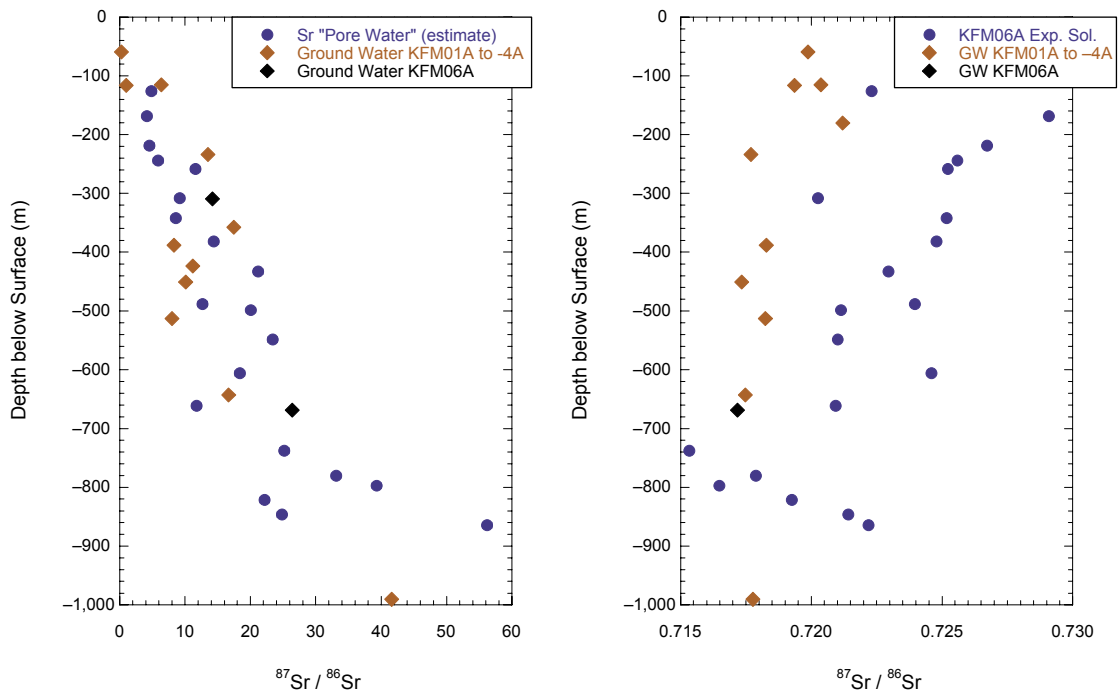
Figure 6-3. *Vertical depth estimate of strontium concentrations in rock pore water from borehole KFM06A (left) and the strontium isotope ratio of experiment solutions (right) compared with those of formation groundwater sampled from adjacent fractures as a function of sampling depth (GW = groundwater).*

7 Summary and conclusions

Pore water that resides in the pore space between minerals and along grain boundaries in crystalline rocks of low permeability cannot be sampled by conventional groundwater sampling techniques and therefore has to be characterised by applying indirect methods based on drillcore material. Accessible, interconnected pore water has been extracted successfully by laboratory out-diffusion methods using some 20 drillcore samples from borehole KFM06A as part of the Forsmark hydrogeochemical site investigation programme. The objective was to characterise these waters chemically and isotopically and relate these data to the present and past groundwater evolution of the site. In addition, the method of extraction, together with interfaced measurements of interconnected porosity, provides the opportunity to derive diffusion coefficient values of potential use in predicting future rates of solute transport. Because of the very small volumes of pore water extracted, and the possibility of rock stress release occurring during drilling which might lead to contamination by drilling fluid and also affect the derivation rock porosity values, great care was taken to avoid such problems or, at least further understand the repercussions.

The study resulted in the following main conclusions:

- the application of indirect methods for pore water extraction and characterisation has been successful,

- the large logistic effort involved in sampling, sample preservation and rapid transport to the laboratory was worthwhile and the quality of the study is largely due to the success of fulfilling these sample requirements,

- independent derivation of water content (to calculate water content porosity) by drying and isotope diffusive exchange methods gave consistent results,

- there is no obvious indication for stress release and its potential effect on water content porosity values and related drilling water contamination; although quantitative proof cannot be given with the present data at hand, several qualitative arguments against such events happening have been discussed,

- the uncertainties surrounding the possibility of stress release effects were addressed by calculating the hypothetical variation in water content using a change of 50% by stress release; this would essentially increase the pore water chloride by a factor of 2,

- diffusion between rock pore water and adjacent water-conducting fractures and fracture zones, and *vice versa*, is identified as the dominant transport process; calculated diffusion coefficients agree with present-day knowledge from the Forsmark site,

- chemical and isotopic pore water signatures are characteristic and show a variation of composition with depth comprising mainly three zones: shallow (Na-Ca-HCO$_3$-Cl type: < 260 m), intermediate (higher concentrations of Ca, Na, and Cl: 260–700 m) and deep (Ca-Na-Cl type: > 700 m); this is in close agreement with the general trends in hydrochemistry of the adjacent formation groundwaters,

- different species appear to be in steady state with formation groundwaters at different depth intervals ($\delta^{18}O$ at intermediate depths; Cl and $\delta^{37}Cl$ and Sr-isotope at greater depths).

8   Acknowledgements

9 References

Claesson L-Å, Nilsson G, 2005. Forsmark site investigation. Drilling of the telescopic borehole KFM06A and the core drilled borehorehole KFM06B at drill site DS6. SKB P-05-50. Svensk Kärnbränslehantering AB.

Chryssanthakis P, 2005. Written comm.

Crank J, 1975. The mathematics of diffusion. Oxford University Press, 2nd edition.

Desaulniers D E, Kaufmann R S, Cherry J A, Bentley H W, 1986. ^{37}Cl-^{35}Cl variations in a diffusion-controlled groundwater system. Geochim. Cosmochim. Acta 50, 1757–1764.

Eggenkamp H G M, Middelbourg J J, Kreulen R, 1994. Preferential diffusion of ^{35}Cl relative to ^{37}Cl in sediments of Kau Bay, Halmahera, Indonesia. Chem. Geol. 116, 317–325.

Frape S K, Fritz P, 1987. Geochemical Trends for Groundwaters from the Canadian Shield. *In*: P. Fritz and S.K. Frape (Eds.), Saline water and gases in crystalline rocks. Geological Association of Canada Special Papers, 19–38.

Gimmi T, Waber H N, 2003. Modelling of profiles of stable water isotopes, chloride and chlorine isotopes of pore water in argillaceous rocks in the Benken borehole. Unpubl. Nagra Internal Report, Wettingen, Switzerland.

Horita J, Wesolowski D J, Cole D R, 1993. The activity-composition relationship of oxygen and hydrogen isotopes in aqueous salt solutions: I. Vapor-liquid water equilibration of single salt solutions from 50 to 100°C. Geochim. Cosmochim. Acta 57**,** 2797–2817.

Horseman S T, Higgo J J W, Alexander J, Harrington F J, 1996. Water, gas and solute movement through argillaceous media. OECD Nuclear Energy Agency, Paris.

Laaksoharju M, Tullborg E-L, Wikberg P, Wallin B, Smellie J A T, 1999. Hydrogeochemical conditions and evolution of the Äspö HRL, Sweden. Appl. Geochem., 14, 819–834.

Laaksoharju M (Ed), 2005. Hydrogeochemical evaluation of the Forsmark site, model version 1.2. SKB R-05-17, Svensk Kärnbränslehantering AB.

Löfgren M, 2004. Diffusive properties of granitic rocks as measured by in situ electrical methods. PhD Thesis, KTH Royal Insititute of Technology, Departement of Chemical Engineering and Technology, Stockholm.

Mattsson H, Keisu M, 2005. Forsmark site investigation: Interpretation of geophysical borehole measurements from KFM06A and HFM20, HFM21 and HFM22. SKB P-05-51. Svensk Kärnbränslehantering AB.

Nagra, 2002. Projekt Opalinuston: Synthese der geowissenschaftlichen Untersuchungs-ergebnisse. Nagra Technical Report NTB 02-03, Wettingen, Switzerland.

Pearson F J, 1987. Models of Mineral Controls on the Composition of Saline Groundwaters of the Canadian Shield. *In*: P. Fritz and S.K. Frape (eds.), Saline water and gases in crystalline rocks. Geological Association of Canada Special Papers, 39–51.

Pearson F J, 1999. What is the porosity of a mudrock? *In: Aplin, A.C., Fleet, A.J., and Macquaker, J.H.S., (Eds.)*, Muds and Mudstones: Physical and Fluid Flow Properties. London, Geol. Soc. Spec. Publ. 158, 9–21.

Pearson F J, Arcos D, Bath A, Boisson J-Y, Fernández A M, Gäbler H-E, Gaucher E, Gautschi A, Griffault L, Hernán P, Waber H N, 2003. Mont Terri Project – Geochemistry of Water in the Opalinus Clay Formation at the Mont Terri Laboratory. Reports of the Federal Office of Water and Geology (FOWG), Geology Series No. 5, Bern, Switzerland.

Rogge T, 1997. Eine molekular-diffusive Methode zur Bestimmung des Porenwassergehaltes und der Zusammensetzung von stabilen Isotopen im Porenwasser von Gestein. Unpubl. Diploma Thesis, Institut für Umweltphysik, Unversity of Heidelberg.

Rouhianen P, Sokolnicki M, 2005. Forsmark site investigation: Difference flow logging in borehole KFM06A. SKB P-05-15. Svensk Kärnbränslehantering AB.

Rübel A P, 2000. Stofftransport in undruchlässigen Gesteinsschichten – Isotopenuntersuchungen im Grund- und Porenwasser. PhD Thesis, Institut für Umweltphysik, Unversity of Heidelberg, Der Andere Verlag, Osnabrück, Germany.

Rübel A P, Sonntag Ch, Lippmann J, Pearson F J, Gautschi A, 2002. Solute transport in formations of very low permeability: Profiles of stable isotope and dissolved noble gas contents of pore water in the Opalinus Clay, Mont Terri, Switzerland. Geochim. Cosmochim. Acta, 1311–1321.

Sacchi E, Michelot J-L, 2000. Pore water Extraction from Argillaceous Rocks for Geochemical Characterisation. Methods and Interpretation. Paris, OECD Nuclear Energy Agency.

Sacchi E, Michelot J-L, Pitsch H, Lalieux P, Aranyossy F-J, 2001. Extraction of water and solutes from argillaceous rocks for geochemical characterisation: Methods, processes, and current understanding. Hydrogeology Journal, 9, 17–33.

SKB, 2001. Site investigations. Investigation methods and general execution programme. SKB TR-01-29. Svensk Kärnbränslehantering AB.

Smellie J A T, Waber H N, Frape S K, 2003. Matrix fluid chemistry experiment, Final Report. SKB TR-03-18. Svensk Kärnbränslehantering AB.

Waber H N, Smellie J A T, 2004. Oskarshamn site investigations Borehole KSH02: Characterisation of matrix pore water (Feasibility Study). SKB P-04-249. Svensk Kärnbränslehantering AB.

Wacker P, Berg C, Nilsson A-C, 2005. Chemical characterisation in borehole KFM06A. Results from the investigated sections at 353.5–360.6 and 768.0–775.1 m. SKB P-05-178. Svensk Kärnbränslehantering AB.

Pore-water data Forsmark borehole KFM06A

Table A1. Bulk and grain density and physical porosity of samples from borehole KFM06A.

Laboratory sample no	Bulk density dry [1], (g/cm³)	Grain density[2] (g/cm³)	Physical porosity, (vol %)	Mass of sample, (g)	Bulk density wet [3], (g/cm³)
KFM06A-1				1,010.668	2.64
KFM06A-2				1,005.660	2.64
KFM06A-3				1,030.279	2.65
KFM06A-4				1,002.994	2.65
KFM06A-5				1,011.977	2.64
KFM06A-6				992.700	2.64
KFM06A-7	2.655	2.667	0.44	1,014.740	2.64
KFM06A-8				1,010.420	2.64
KFM06A-9				993.992	2.59
KFM06A-10				1,011.830	2.65
KFM06A-11				1,017.305	2.65
KFM06A-12	2.696	2.705	0.34	1,036.810	2.68
KFM06A-13				1,009.386	2.64
KFM06A-14				1,031.290	2.63
KFM06A-15	2.665	2.672	0.27	1,008.946	2.65
KFM06A-16				987.028	2.60
KFM06A-17				1,004.066	2.61
KFM06A-18				999.525	2.63
KFM06A-19				1,004.835	2.63
KFM06A-20				1,002.250	2.62
KFM06A-21				997.045	2.62
KFM06A-22				995.352	2.63
KFM06A-23				999.720	2.62

[1] determined by Hg-displacement on dry rock sample,
[2] determined by He-pycnometry on dry rock sample,
[3] determined from mass and volume of saturated (wet) drillcore sample used for out-diffusion experiment.

Table A2. Average water content by drying at 105°C and water-content porosity of rock samples from borehole KFM06A.

Laboratory sample no	Number of samples	Water content average, (wt %)	Water content 1 σ, (wt %)	WC-porosity average, (vol %)	WC-porosity 1 σ, (vol %)
KFM06A-1	3	0.182	0.047	0.478	0.123
KFM06A-2	3	0.219	0.016	0.576	0.042
KFM06A-3	3	0.150	0.022	0.397	0.059
KFM06A-4	3	0.183	0.028	0.484	0.075
KFM06A-5	3	0.117	0.010	0.308	0.025
KFM06A-6	3	0.303	0.052	0.798	0.136
KFM06A-7	3	0.121	0.007	0.319	0.018
KFM06A-8	3	0.111	0.021	0.292	0.056
KFM06A-9	3	0.165	0.016	0.426	0.040
KFM06A-10	3	0.120	0.008	0.316	0.020
KFM06A-11	3	0.106	0.012	0.281	0.033
KFM06A-12	3	0.110	0.012	0.293	0.033
KFM06A-13	3	0.113	0.008	0.298	0.022
KFM06A-14	3	0.078	0.007	0.205	0.017
KFM06A-15	3	0.112	0.005	0.295	0.014
KFM06A-16	3	0.121	0.007	0.315	0.018
KFM06A-17	3	0.098	0.011	0.255	0.028
KFM06A-18	3	0.117	0.013	0.306	0.034
KFM06A-19	3	0.105	0.017	0.275	0.043
KFM06A-20	3	0.081	0.023	0.212	0.061
KFM06A-21	3	0.136	0.011	0.356	0.028
KFM06A-22	3	0.230	0.020	0.603	0.051
KFM06A-23	3	0.107	0.018	0.279	0.048

Table A3. $\delta^{18}O$ and δ^2H of standard solutions used for the isotope diffusive exchange method and the out-diffusion experiments.

Standard no	Date	$\delta^{18}O$ ‰ V-SMOW	δ^2H ‰ V-SMOW	Isotope diffusive exchange samples KFM06A-	Out-diffusion samples KFM06A-
STD-LAB 1	16.06.2004	−11.13	−78.2		
STD-LAB 2	24.06.2004	−11.20	−80.6	1, 2, 4	
STD-LAB 3	21.07.2004	−11.05	−78.1	3, 5–8	
STD-LAB 4	04.09.2004	−11.94	−84.2	9–15	
STD-LAB 5	25.09.2004	−11.32	−80.0		
STD-LAB 6	25.09.2004	−11.14	−79.2	16–23	
STD-TEW 1	16.06.2004	−109.76	425.5		
STD-TEW 2	24.06.2004	−109.79	425.7	1, 2, 4	1, 2, 4
STD-TEW 3	21.07.2004	−109.86	425.5	3, 5–8	3, 5–8
STD-TEW 4	04.09.2004	−109.85	425.8	9–15	9–15
STD-TEW 5	25.09.2004	−109.84	425.3		
STD-TEW 6	25.09.2004	−109.68	426.9	16–23	16–23

Table A4. $\delta^{18}O$ and δ^2H of pore water and water content derived from isotope diffusive exchange method.

Laboratory sample no	Average vertical depth (m)	$\delta^{18}O^{1)}$ pore water (‰ V-SMOW)	$\delta^2H^{1)}$ pore water (‰ V-SMOW)	Water Content$^{1)}$ (wt-%)
KFM06A-1	126.50	−10.43	−90.4	0.232
KFM06A-2	168.62	−14.94	−96.9	0.180
KFM06A-3	218.59	−10.67	1.1	0.196
KFM06A-4	244.06	−10.32	−66.5	0.188
KFM06A-5	258.50	−8.65	−44.5	0.15
KFM06A-6	307.69	−9.74	−12.3	0.357
KFM06A-7	342.38	−10.70	−29.7	0.121
KFM06A-8	381.90	3.05	57.3	0.134
KFM06A-9	433.03	−8.32	−72.6	0.168
KFM06A-10	487.90	−8.36	−35.3	0.145
KFM06A-11	498.78	−6.83	6.2	0.159
KFM06A-12	514.96	n.a.	n.a.	
KFM06A-13	548.68	−8.57	−34.6	0.098
KFM06A-14	572.35	n.a.	n.a.	
KFM06A-15	603.46	−7.04	−25.7	0.199
KFM06A-16	661.29	−7.44	25.4	0.136
KFM06A-17	702.21	−9.37	−29.5	0.115
KFM06A-18	737.60	−8.73	26.0	0.122
KFM06A-19	780.26	−8.65	−28.5	0.135
KFM06A-20	797.34	−5.16	5.8	0.115
KFM06A-21	821.66	−10.39	−66.2	0.113
KFM06A-22	846.42	−9.94	−56.0	0.210
KFM06A-23	864.57	−6.98	−71.1	0.204

[1] data in italics (rastered areas) are not reliable and not used for further interpretation due to: a) experimental artefacts ($\delta^{18}O$ and δ^2H, evaporation), and b) analytical artefacts (only δ^2H, memory effect during ^2H mass spectrometric measurements).

Table A5. Chemical composition of solutions from out-diffusion experiments at steady state conditions.

Out-diffusion experiment solution	Units	KFM06A-1	KFM06A-2	KFM06A-3	KFM06A-4	KFM06A-5	KFM06A-6	KFM06A-7	KFM06A-8	KFM06A-9
SAMPLE DESCRIPTION										
Vertical Depth	m	126.50	168.47	218.59	244.06	258.50	307.69	342.38	381.90	433.03
Rock Type										
Water-Rock Ratio		0.107	0.092	0.100	0.109	0.099	0.107	0.102	0.106	0.100
Experiment Temperature	°C	20	45	45	45	45	45	45	45	45
Experiment Time	days	172	99	92	99	92	92	92	92	90
MISC. PROPERTIES										
Chemical Type		Na-Ca-HCO$_3$-Cl-F	Na-Ca-HCO$_3$-Cl	Na-Ca-HCO$_3$-(Cl)	Na-Ca-HCO$_3$-Cl	Na-Ca-HCO$_3$-Cl	Na-Ca-HCO$_3$-Cl	Na-Ca-HCO$_3$-Cl	Na-Ca-HCO$_3$-Cl	Na-Ca-HCO3-Cl-F
pH (lab)	-log(H+)	7.28	7.21	7.57	7.08	6.91	7.35	7.47	7.31	7.12
Electrical Conductivity	µS/cm	283	327	247	241	265	444	286	315	461
Sample Temperature	°C	20	20	20	20	20	20	20	20	20
CATIONS										
Sodium (Na$^+$)	mg/L	46.9	43.5	40.3	42.3	38.1	58.2	47.3	42	40.4
Potassium (K$^+$)	mg/L	2.9	4.5	4	3.3	3.8	3.5	4.3	3.4	3.7
Magnesium (Mg^{+2})	mg/L	0.9	0.7	< 0.5	0.6	0.6	1.3	0.6	0.8	0.5
Calcium (Ca^{+2})	mg/L	11	21	12.8	11	17.4	41.7	20.2	30.1	50
Strontium (Sr^{+2})	mg/L	0.058	0.13	0.081	0.098	0.15	0.28	0.15	0.17	0.31
ANIONS										
Fluoride (F$^-$)	mg/L	6.2	3.3	1.8	3.8	3.3	2.5	1.7	2.3	3.7
Chloride (Cl$^-$)	mg/L	27.4	33.6	12.3	15.5	25.1	42.8	22	27.4	53.2
Bromide (Br$^-$)	mg/L	< 0.1	< 0.1	< 0.1	< 0.1	< 0.1	< 0.1	< 0.1	< 0.1	0.23
Sulfate (SO$_4^{-2}$)	mg/L	9.9	8.4	5.2	7.3	5.7	8.8	2.8	5.1	7
Nitrate (NO$_3^-$)	mg/L	< 0.5	< 0.5	1.6	< 0.5	< 0.5	2.2	< 0.5	< 0.5	< 0.5
Total Alkalinity as HCO$_3^-$	mg/L	81.8	85.4	104.9	75.1	69.6	145.8	105.6	105.6	133.6
CALC. PARAMETERS										
Total dissolved solids	mg/L	186	200	181	158	163	304	204	216	292
Charge Balance	%	1.73	7.22	4.18	11.13	11.11	9.90	12.75	12.15	4.29

Table A5. (continued).

Out-diffusion experiment solution	Units	KFM06A-10	KFM06A-11	KFM06A-12	KFM06A-13	KFM06A-14	KFM06A-15	KFM06A-16	KFM06A-17	KFM06A-18
SAMPLE DESCRIPTION										
Vertical Depth	m	487.90	498.78	514.87	548.68	572.35	606.05	661.29	702.21	737.60
Rock Type										
Water-Rock Ratio		0.105	0.103	0.101	0.106	0.102	0.112	0.106	0.103	0.101
Experiment Temperature	°C	45	45	45	45	45	45	20	45	45
Experiment Time	days	90	90	90	90	90	90	149	89	89
MISC. PROPERTIES										
Chemical Type		Na-Ca-$\underline{HCO_3}$-Cl	Na-Ca-$\underline{HCO_3}$-Cl		Na-Ca-HCO_3-Cl		Na-Ca-HCO_3-Cl	Na-Ca-$\underline{HCO_3}$-Cl		$\underline{Ca}$-Na-Cl-HCO_3
pH (lab)	-log(H+)	6.92	7.11	7.23	7.17	7.03	7.05	7.74	6.35	6.49
Electrical Conductivity	µS/cm		352				327			
Sample Temperature	°C	20	20	20	20	20	20	20	20	20
CATIONS										
Sodium (Na$^+$)	mg/L	43.1	45.2		42.2		37.8	31.8		31.7
Potassium (K$^+$)	mg/L	3.6	3.5		3.8		3.5	2.2		1.6
Magnesium (Mg^{+2})	mg/L	0.5	< 0.5		0.5		< 0.5	< 0.5		0.5
Calcium (Ca^{+2})	mg/L	25.6	23.5		37.1		24.1	20.3		39.9
Strontium (Sr^{+2})	mg/L	0.12	0.16		0.21		0.16	0.1		0.28
ANIONS										
Fluoride (F$^-$)	mg/L	2.4	4.9		2.9		5.3	2		2
Chloride (Cl$^-$)	mg/L	25.2	36.4		44.2		39.1	31.7		60.4
Bromide (Br$^-$)	mg/L	< 0.1	< 0.1		0.28		< 0.1	0.53		0.52
Sulfate (SO$_4^{-2}$)	mg/L	7.4	7.4		7.6		7.2	3.7		13.6
Nitrate (NO$_3^-$)	mg/L	< 0.5	< 0.5		< 0.5		< 0.5	< 0.5		< 0.5
Total Alkalinity as HCO$_3^-$	mg/L	98.2	93.4	111.1	123.3	78.7	67.7	83.6	51.9	55.5
CALC. PARAMETERS										
Total dissolved solids	mg/L	206	214		261		185	175		205
Charge Balance	%	11.66	4.25		3.36		5.34	0.03		6.95

Table A5. (continued).

Out-diffusion experiment solution	Units	KFM06A-19	KFM06A-20	KFM06A-21	KFM06A-22	KFM06A-23	Standard solution
SAMPLE DESCRIPTION							
Vertical Depth	m	780.26	797.34	821.66	846.42	864.58	
Rock Type							
Water-Rock Ratio		0.101	0.101	0.106	0.102	0.101	
Experiment Temperature	°C	45	20	45	45	45	
Experiment Time	days	89	149	89	89	89	
MISC. PROPERTIES							
Chemical Type		Na-Ca-Cl-HCO$_3$	Ca-Na-Cl-HCO$_3$	Ca-Na-Cl-HCO$_3$	Ca-Na-Cl-HCO$_3$	Ca-Na-Cl-HCO$_3$	
pH (lab)	-log(H+)	7.27	7.4	7.19	7.23	6.1	
Electrical Conductivity	µS/cm	340				459	14
Sample Temperature	°C	20	20	20	20	20	20
CATIONS							
Sodium (Na$^+$)	mg/L	37.9	30.7	30.7	70.9	47.3	0.2
Potassium (K$^+$)	mg/L	2.1	1.5	2.1	3.4	2.9	< 0.1
Magnesium (Mg^{+2})	mg/L	< 0.5	0.5	0.5	0.5	< 0.5	0.3
Calcium (Ca^{+2})	mg/L	32.3	37.5	38.3	66.8	53	0.1
Strontium (Sr^{+2})	mg/L	0.31	0.28	0.28	0.51	0.6	
ANIONS							
Fluoride (F$^-$)	mg/L	3.5	0.9	2.2	2.2	3.5	< 0.1
Chloride (Cl$^-$)	mg/L	75.7	79.1	82.1	145	122	1.1
Bromide (Br$^-$)	mg/L	0.4	0.15	1.3	1	0.64	< 0.1
Sulfate (SO$_4^{-2}$)	mg/L	5.9	4.8	3.8	7.5	10.8	< 0.1
Nitrate (NO$_3^-$)	mg/L	0.9	1.5	< 0.5	0.9	< 0.5	
Total Alkalinity as HCO$_3^-$	mg/L	56.7	48.8	50.0	85.4	43.9	< 0.1
CALC. PARAMETERS							
Total dissolved solids	mg/L	214	204	210	382	284	< 2
Charge Balance	%	−1.05	1.73	0.01	6.35	2.26	2.57

Table A6. Isotopic composition of solutions from out-diffusion experiments at steady state conditions.

Laboratory sample no	Average vertical depth (m)	δ¹⁸O[1] ‰ V-SMOW	δ²H[1] ‰ V-SMOW	δ³⁷Cl ‰ V-SMOC	Sr ppm	⁸⁷Sr /⁸⁶Sr	⁸⁷Sr /⁸⁶Sr 1 σ
KFM06A-1	126.50			0.51	0.082	0.722315	0.000042
KFM06A-2	168.62	−6.7	82	0.97	0.108	0.729086	0.000022
KFM06A-3	218.59	24.7	−115	1.31	0.068	0.726727	0.00002
KFM06A-4	244.06	20.5	−117	1.85 [2]	0.097	0.725589	0.000032
KFM06A-5	258.50	79.8	−462	0.62	0.135	0.725231	0.000020
KFM06A-6	307.69	7.8	−203	0.17	0.252	0.720257	0.000020
KFM06A-7	342.38	86.6	−698	1.04	0.100	0.725174	0.000032
KFM06A-8	381.90	82.1	−1,011	0.75	0.149	0.724792	0.000020
KFM06A-9	433.03	n.a.	n.a.	1.01	0.343	0.722954	0.000021
KFM06A-10	487.90	n.a.	n.a.	0.59	0.142	0.723958	0.000020
KFM06A-11	498.78	n.a.	n.a.	b.d.[3]	0.204	0.721135	0.000021
KFM06A-12	514.96	n.a.	n.a.				
KFM06A-13	548.68	n.a.	n.a.	b.d.[3]	0.248	0.721013	0.000020
KFM06A-14	572.35	n.a.	n.a.				
KFM06A-15	606.05	n.a.	n.a.	3.26	0.182	0.724597	0.000020
KFM06A-16	661.29	n.a.	n.a.	0.48	0.134	0.720926	0.000020
KFM06A-17	702.21	n.a.	n.a.				
KFM06A-18	737.60	n.a.	n.a.	0.36	0.289	0.715329	0.000020
KFM06A-19	780.26	n.a.	n.a.	0.43	0.340	0.717890	0.000022
KFM06A-20	797.34	n.a.	n.a.	0.13	0.311	0.716483	0.000020
KFM06A-21	821.66	n.a.	n.a.	0.15	0.282	0.719254	0.000020
KFM06A-22	846.42	n.a.	n.a.	0.10	0.550	0.721426	0.000020
KFM06A-23	864.57	n.a.	n.a.	0.79	0.587	0.722194	0.000020

[1] calculated data in italics are meaningless and not used for further interpretation (see text for explanation),
[2] very small signal, not used for further interpretation,
[3] too low chloride content for isotope analysis.

Table A7. Chloride concentration of pore water calculated from out-diffusion solutions and the water content of the samples.

Laboratory sample no	Average vertical depth (m)	Pore water Cl mg/kg H$_2$O	Pore water Cl + error mg/kg H$_2$O	Pore water Cl – error mg/kg H$_2$O
KFM06A-1	126.50	1,563	532	314
KFM06A-2	168.62	1,256	96	83
KFM06A-3	218.59	759	130	97
KFM06A-4	244.06	822	148	109
KFM06A-5	258.50	2,070	182	155
KFM06A-6	307.69	1,460	292	207
KFM06A-7	342.38	1,923	113	101
KFM06A-8	381.90	2,516	591	401
KFM06A-9	433.03	3,038	314	259
KFM06A-10	487.90	2,036	138	122
KFM06A-11	498.78	3,466	454	359
KFM06A-12	514.96			
KFM06A-13	548.68	3,855	300	260
KFM06A-14	572.35			
KFM06A-15	606.46	3,830	186	169
KFM06A-16	661.29	2,558	149	133
KFM06A-17	702.21			
KFM06A-18	737.60	4,886	607	485
KFM06A-19	780.26	6,870	1,277	928
KFM06A-20	797.34	9,304	3,777	2,076
KFM06A-21	821.66	6,044	512	437
KFM06A-22	846.42	6,139	561	473
KFM06A-23	864.57	11,382	2,349	1,657

Shaded area: Pore-water Cl concentrations of these samples are preliminary and will change to slightly higher values (approx 5%) because Cl time series samples not yet analysed. Therefore, values are only corrected for the mass removed by Cl time series sampling, but not for the Cl removed by these samples (see text for explanation).